Theoretical Studies of the Dependence of Chemical Reaction on Tautomeric Form of His64 in the Active Site of Human Carbonic Anhydrase Ⅱ

メタデータ	言語: eng 出版者: 公開日: 2017-10-05 キーワード (Ja): キーワード (En): 作成者: メールアドレス: 所属:
URL	http://hdl.handle.net/2297/40524

This work is licensed under a Creative Commons Attribution-NonCommercial-ShareAlike 3.0 International License.

Theoretical Studies of the Dependence of Chemical Reaction on Tautomeric Form of His64 in the Active Site of Human Carbonic Anhydrase II

Muhamad Koyimatu

July 4th

2014

Dissertation

Theoretical Studies of the Dependence of Chemical Reaction on Tautomeric Form of His64 in the Active Site of Human Carbonic Anhydrase II

ヒト由来炭酸脱水酵素 II の化学反応性の活性部位 His64 互変異性依存性に関する理論的研究

Graduate School of Natural Science and Technology
Kanazawa University

Major Subject: Mathematical and Physical Sciences
Course: Computational Science

1123102011
Name: Muhamad Koyimatu
Chief Advisor: Hidemi Nagao

Acknowledgement

This doctoral thesis is a summary of my research from October 2011 to June 2014 at Graduate School of Natural Science and Technology, Kanazawa University.

I would like to convey my gratefulness to Professor Hidemi Nagao for the guidance, discussion, and encouragement throughout the course of this thesis. I also want to express a deep sense of gratitude to Professor Hideto Shimahara at Japan Advanced Institute of Science and Technology for various discussion and advices. I would like to thank Dr. Hiroaki Saito, Dr. Kazutomo Kawaguchi, and Dr. Kimikazu Sugimori.

The financial support of the Asahi Glass Scholarship Foundation is gratefully acknowledged.

Lastly, I thank almighty, my family, friends, and colleagues for their constant encouragement.

Contents

Acknowledgement ii

Contents iv

Part I. General Introduction 1

1 Introduction to the Thesis 3

1.1. Assessing Properties of Amino Acid Residues on Human Carbonic Anhydrase II 3

1.2. The energy profile of tautomeric forms and imidazolium form of His64 on Human Carbonic Anhydrase 4

1.3. The interaction energy profile of tautomeric forms and imidazolium form of His64 on Human Carbonic Anhydrase 4

2 Introduction to Studies on Carbonic Anhydrase and *ab initio* calculation............5

2.1 Carbonic Anhydrase 5

2.2 Human Carbonic Anhydrase II 7

2.3 Hydrogen bonding Interaction 8

3 Ab initio calculation 11

3.1 Density Functional Theory 11

3.2 Møller-Plesset Perturbation Theory 15

3.3 Hybrid Meta-generalized gradient-approximation (hybrid meta-GGA) exchange functional 17

Part II. The Properties of Carbonic Anhydrase 21

4 The π-stacking interaction between Trp5 and His64 on Human Carbonic Anhydrase II 23
4.1 Introduction 23
4.2 Computational Details 24
4.3 Result and Discussion 26
4.3.1 Method and basis set comparison 26
4.3.2 Substitution of Imidazole with Benzene 28
4.4 Conclusions 30
5 Tautomeric forms of His64 and The Difference Energies 31
5.1 Introduction 31
5.2 Computational Details 32
5.3 Results and Discussion 34
5.3.1 The Energy Profile of B3LYP Method 34
5.3.2 The Energy Profile using MP2 method 37
5.4 Conclusion 40
6 Interaction energy of Trp5 to Tautomeric forms and imidazolium ion of His64 41
6.1 Computational Details 41
6.2 Results and Discussion 43
6.2.1 M06-2X calculation 43
6.2.2 MP2 calculation 46
6.3 Conclusion 49
Part III. General Conclusions 51

7 General Conclusion 53
  7.1 The π-stacking interaction to His64 53
  7.2 Potential Energy Profile 53
  7.3 The Interaction Energy Profile 53
  7.4 Future works 54
Appendix 55
Appendix A. Approaching Proton Relay in Human Carbonic Anhydrase II 57
  A.1 Introduction 57
  A.2 Computational Details 58
  A.3 Results and Discussion 60
    A.3.1 Geometry Optimization 60
    A.3.2 Potential energy profiles 62
  A.4 Conclusion 64
List of Publications 65
References 67

Part I. General Introduction

1 Introduction to the Thesis

This doctoral thesis is a summary of my research interest in carbonic anhydrase. The big determination was used to the structural, energetic, and interaction of residues in carbonic anhydrase.

Three years of my research at Graduate School of Natural Science and Technology Kanazawa University between October 2011 and June 2014 can be summarized in the three steps, based on my three publications as the first author.

1.1. Assessing Properties of Amino Acid Residues on Human Carbonic Anhydrase II

We have investigated the presence of the π-stacking interaction that could stabilize the local structure of protein by using the density functional theory (DFT) and second order of Møller-Plesset Perturbation theory (MP2) calculation to understand the structural geometry of human carbonic anhydrase II.

M. Koyimatu, H. Shimahara, M. Iwayama, K. Sugimori, K. Kawaguchi, H. Saito, and H. Nagao, *Theoretical Model For Assessing Properties of Local Structures in Metalloprotein*, American Institute of Physics AIP Conference Proceeding, Volume 1518, pp. 626-629 (2013).

1.2. The energy profile of tautomeric forms and imidazolium form of His64 on Human Carbonic Anhydrase

We have investigated the difference energy and energy profile for Nε2-H tautomeric form of His64 on Human carbonic anhydrase II by using MP2 method. The energy profile at the "out" region is stabilized by π-stacking interaction.

Muhamad Koyimatu, Hideto Shimahara, Kazutomo Kawaguchi, Hirosaki Saito, Kimikazu Sugimori, and Hidemi Nagao, *Theoretical Study of a π-stacking interaction in carbonic anhydrase,* Recent Development in Computational Science, Volume 4, pp. 87-93 (2013).

1.3. The interaction energy profile of tautomeric forms and imidazolium form of His64 on Human Carbonic Anhydrase

We have investigated the interaction energy in of the addition of Trp5 to His64 by applying binding energy equation and counterpoise method. We applied the M06-2X, a better DFT theory than B3LYP theory for geometry optimization.

Muhamad Koyimatu, Hideto Shimahara, Kimikazu Sugimori, Kazutomo Kawaguchi, Hirosaki Saito, and Hidemi Nagao, *π-stacking Interaction between Heterocyclic Rings in a Reaction Field of Biological System,* The Physical Society of Japan JPS Conference Proceeding, Volume 1 (2014).

2 Introduction to Studies on Carbonic Anhydrase and *ab initio* calculation

2.1 Carbonic Anhydrase

Carbonic anhydrase (CA) are enzymes that helps regulate the acid-base balance and pH in blood and other animal tissues. It is known for its role in facilitating the transport of carbon dioxide and protons in the intracellular space, across biological membranes and in the layers of the extracellular space. This enzyme is present in most organisms, from bacteria to plant.

CA was first discovered in vertebrate erythrocytes [1]. It was found that a catalyst was present in blood that could dehydrate bicarbonate and allow it to escape as CO_2 [2]. The first CA was purified from erythrocytes in 1933 followed by characterization of several mammalian isozymes [3]. The existence of CA in plant has been discovered in 1947 [4], however cannot overcome the domination of CA research in mammalian until recently.

Carbonic anhydrase (CA) catalyze the reversible reaction between carbon dioxide hydration and bicarbonate dehydration, by the following reaction [5].

$$H_2O + CO_2 \rightleftharpoons H^+ + HCO_3^- \tag{2.1}$$

CA was found to contain bound zinc, associated with catalytic activity. This discovery made carbonic anhydrase the first known zinc-containing enzymes [6]. The zinc-hydroxide mechanism is widely accepted to explain the role of zinc ion in by two-step mechanisms [7, 8]. In the first step, the zinc-bound hydroxide bind to the carbon dioxide to form the zinc bound bicarbonate. The bicarbonate of this

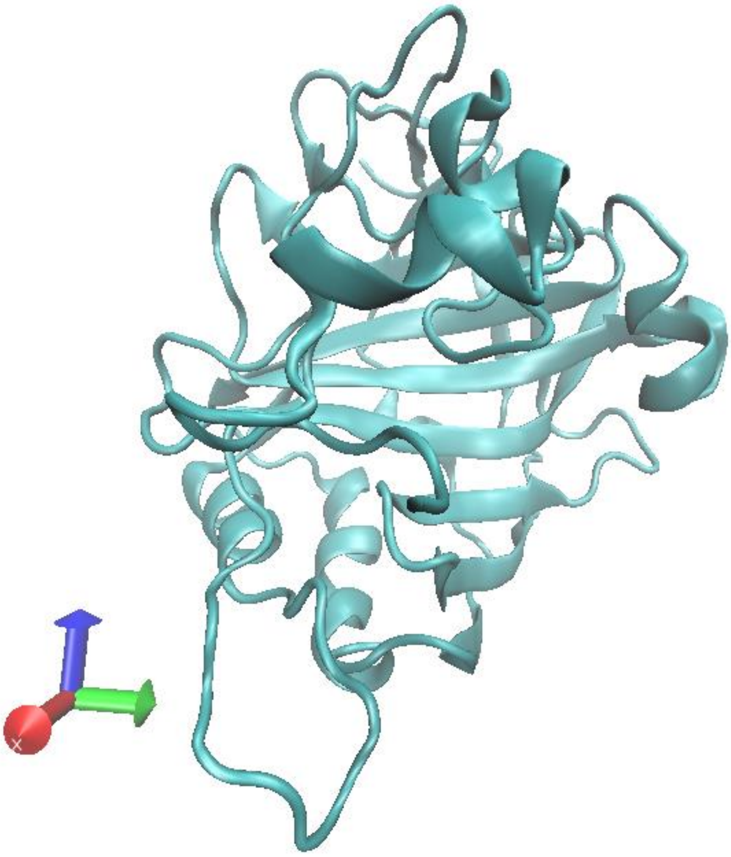

Figure 1. Visualization of HCAII (PDB file, code: 2CBA)

intermediate is replaced by a water molecule. In the second step, the active site is regenerated by the ionization of the zinc-bound water molecules and transferring a proton to an exogenous proton acceptor such as buffer (B) solution, equation (2.3).

$$EZnOH^{-} + CO_2 + H_2O \rightleftharpoons HCO_3^{-} + EZn\text{-}H_2O \tag{2.2}$$

$$EZnH_2O + B \rightleftharpoons EZnOH^{-} + BH^{+} \tag{2.3}$$

2.2 Human Carbonic Anhydrase II

Human Carbonic Anhydrase II (HCAII) has the fastest catalytic rate among CA isozymes [9, 10]. For HCAII, Histidine at position 64 (His64) has been considered to mediate the transfer of proton from zinc-bound water to a buffer molecule (Equation 2.3). Replacing it with another residue could drastically decrease the maximal turnover rate [11, 12]. X-ray crystallography data shows that the active site of HCAII has two orientations of His64 and water-bridge that connected the zinc-bound water and His64 [13]. The two orientation of His64 (“in” and “out” conformation) has been assumed to be related to the swinging or rotational motion of His64 as a final step of the proton transfer.

Due to the weakness of diffraction signal, the hydrogen atoms position and occupancies cannot be easily obtained by X-ray crystallography. Increasing the X-ray dose cannot enhanced the signal of hydrogen atom easily [14]. The position of hydrogen atom is important is necessary to determine the form of His64 (Nδ1-H tautomer, Nε2-H tautomer, or protonated form). The position of hydrogen atom can be determined by using NMR information data of HCAII. The NMR study also suggest that the interconversion of two tautomeric form and one protonated form can be associated with the proton transfer [15]. It believed that two alternate conformation has a relation to the rotational motion as a final step of proton transfer.

2.3 Hydrogen bonding Interaction

Hydrogen bond is a noncovalent, attractive interaction between a proton donor and a proton acceptor. Hydrogen bond occurs when H atom is bonded to electronegative atoms such as N, O, and F atoms. However, in the stabilization of weak hydrogen bonding interaction, the C-H can be involved in hydrogen bond and the p electron can act as a proton acceptors [16, 17]. The three types of hydrogen bonding interactions, which are most often discussed, are weak, moderate, and strong. The strength of weak, moderate, and strong hydrogen bonds are vary from 1-4 kcal/mol, 4-15 kcal/mol, 15-40 kcal/mol, respectively [16, 17, 18, 19]. The strength of hydrogen bond is depending on its length and angle and directionality.

Most biological molecules have so many hydrogen bonding group that hydrogen bonding is important in determining their three-dimensional structures and their intermolecular association. The internal hydrogen bonding group of protein are arranged in nearly all possible hydrogen bond are possibility formed. Hydrogen bonds has a major influence on the structures of proteins. In protein, the hydrogen bonding interactions always between C-O and H-N group, that give a shape to alpha helices and beta pleated sheet.

Other than protein, water molecules also associate through hydrogen bonds. The hydrogen bond length between two water molecules is 1.8 Å. This interaction is crucial to both the properties of water and to its role as a biochemical solvent. Water dissolves more types of substances and in greater amount than any other solvent. The polarity of water makes it an excellent solvent for polar and ionic materials.

The dissolve process can be related to Coulomb's law:

$$U = \frac{kq_1q_2}{r} \tag{2.4}$$

Where U is the energy association, q_1 and q_2 are two electronic charges, r is the distance, and k is a proportionality constant. The dielectric constant of a solvent is measured of its ability to keep the opposite charges apart. The dielectric constant of water is among the highest of any pure liquid, whereas those of nonpolar substances, such as hydrocarbons, are relatively small [20].

When electrical current passes an ionic solution, the ion migrate toward the opposite electrodes at a rate, depending on to electrical field and frictional drag of ion and solution. The mobility of H_3O^+ and OH^- are faster compared to other ions [21]. The high mobility rate of H_3O^+ (or H^+, proton) resulting from the ability of protons jump rapidly jumps from water molecule to another water molecules. This proton movement ability also responsible in acid-base reactions in aqueous solution and probably have an important role in biological proton-transfer reactions.

In HCAII, the exceed proton from CO_2 hydration in the active site is transferred to a bulk buffer molecules via His64. The distance between His64 and zinc atom is approximately 7.5 Å, and the proton cannot directly jump at such a long distance. X-ray crystallography shows several water molecules are visible between them. The water molecules form a hydrogen bond network that help the mobilization of proton from the active site to the His64.

3 Ab initio calculation

The development of quantum theory has begun since 20th century. It solved many problems in science with a good precision and accuracy. However the Schrödinger equation, a fundamental equation in quantum mechanics, cannot be solved by analytically, and cannot be applied to large-scale system. To solve a difficult equation, a numerical method is required.

3.1 Density Functional Theory

Density functional theory (DFT) tried to simplify the work to find the energy of a system [22]. In the Hartree-Fock (HF) theory, the position variable of each electron was needed to build a wave function of atom or molecule to determine the energy. The DFT theory tried to approach that system by using one variable, a density function for atom in a space. Thus the energy of a system can be solved easily by computation.

The DFT method was constructed from Hohenberg-Kohn theory, by proposing two theorems [23, 24]. The first theorem states that the ground state of electron density of many electron systems in the presence of an external potential uniquely determines the external potential. The second theorem states that the functional that delivers the ground state energy of the system, delivers the lowest energy if and only the density is true ground state density.

Using both theorem, Kohn and Sham assemble an equation of electron density and energy.

$$E[\rho(r)] = T_{ni}[\rho(r)] + V_{ne}[\rho(r)] + V_{ee}[\rho(r)] + E_{xc}[\rho(r)] \tag{3.1}$$

That equation express that the energy of the system is the total energy of kinetic of electron with the assumption that there is no interaction, potential between nucleus and electron, potential repulsive between electrons, and the correction of the total energy caused by non-classical interaction between electrons. The real system can be approach using this unreal system, because both systems has the same density when the number of atoms and position is same.

With the assumption that no electrons interaction in the unreal system, the kinetic energy for the system can be represented by the total of kinetic energy for each electrons. Energy as a function of density that including electron orbital can be described in equation

$$E[\rho(r)] = \sum_{i}^{N} \left(\langle x_i \left| -\frac{1}{2}\nabla_i^2 \right| x_i \rangle - \langle x_i \left| \sum_{k}^{nuclei} \frac{Zk}{|r_i - r_k|} \right| \rangle \right) + \sum_{i}^{N} \langle x_i \left| \frac{1}{2} \int \frac{\rho(r')}{|r_i - r'|} dr' \right| x_i \rangle + E_{xc}[\rho(r)] \tag{3.2}$$

Density and electron orbital can be associated with

$$\rho = \sum_{i=1}^{N} \langle x_i | x_i \rangle \tag{3.3}$$

E_{xc} is a difference of total energy between real system and unreal system.

That energy equation can be solved by finding the x which minimalize the energy value. If x is constructed by single orbital electron x_i, we can obtain the equation

$$h_i^{KS} x_i = \varepsilon_i x_i \tag{3.4}$$

With the Kohn-Sham operator that can defined as

$$h_i^{KS} = -\frac{1}{2}\nabla_i^2 - \sum_k^{nuclei} \frac{Z_k}{|r_i - r_k|} + \int \frac{\rho(r')}{|r_i - r'|} dr' + V_{xc} \tag{3.5}$$

and

$$V_{xc} = \frac{\delta E_{xc}}{\delta \rho} \tag{3.6}$$

That equation can be solved if the function of *E_{xc}* is known. E_x can be approach by the following equation:

$$\varepsilon_x[\rho(r)] = -\frac{9\alpha}{8}\left(\frac{3}{\pi}\right)^{\frac{1}{3}} \rho^{\frac{1}{3}}(r) \tag{3.7}$$

This approach known as Local Density Approximation (LDA) because equation (3.7) explicitly refer to the ε_c value at a position can be calculated from the density of that position. The value of α can be vary, a=2/3 for LDA method, α=1 for Slater method, and α=3/4 for Xα method.

All method above can be expanded by adding the polarization spin effect, became:

$$\varepsilon_x[\rho(r),\xi] = \varepsilon_x^0[\rho(r)] + \{\varepsilon_x^1[\rho(r)] - \varepsilon_x^0[\rho(r)]\}\left[\frac{(1+\xi)^{4/3} + (1-\xi)^{4/3} - 2}{2(2^{\frac{1}{3}} - 1)}\right] \tag{3.8}$$

that know as Local Spin Density Approximation (LSDA).

Vosko, Wilk, and Nusair (VWN) propose an approach for ε_c that similar with the LSDA [25]. The value for ε_c can be described in equation (3.9).

$$\varepsilon_c^i(r_s) = \frac{A}{2}\left\{ ln\frac{r_s}{r_s + b\sqrt{r_s + c}} + \frac{2b}{\sqrt{4c - b^2}}\tan^{-1}\left(\frac{\sqrt{4c - b^2}}{2\sqrt{r_s + b}}\right) - \frac{bx_0}{x_0^2 + bx_0 + c}\left\{ ln\left[\frac{(\sqrt{r_s} - x_0)^2}{r_s + b\sqrt{r_s} + c}\right] + \frac{2(b - 2x_0)}{\sqrt{4c - b^2}}\tan^{-1}\left(\frac{\sqrt{4c - b^2}}{2\sqrt{r_s} + b}\right)\right\}\right\} \tag{3.9}$$

The most common variation for the ε_c is VNW and VNW5. The combination of ε_c and Slater ε_x is known as SVWN.

In a molecular system, the electron density is not homogenous. A better variable of E_{xc} than LDA and LSDA is needed. A way to obtain a better LSDA value is adding density gradient component to the ε_{xc} value, known as Generalized Gradient Approximation (GGA).

$$\varepsilon_{x/c}^{GGA}[\rho(r)] = \varepsilon_{\frac{X}{C}}^{LSDA}[\rho(r)] + \Delta\varepsilon_{x/c}\left[\frac{\nabla\rho(r)}{\rho^{\frac{4}{3}}(r)}\right] \tag{3.10}$$

Some applications of ε_x GGA function that popular are B, CAM, FT97, etc. The most popular of ε_c GGA function is LYP (Introduced by Lee, Yang, and Parr) [26]. The more advanced function improvement is by adding the component of second derivative density to the ε_{xc} value, known as meta-GGA.

Another approach is by combine the E_x from HF with E_{xc} from DFT. This combination is very famous and well known as B3LYP method, which can be defined as equation (3.11) [27, 28].

$$E_{xc}^{B3LYP} = (1-a)E_x^{LSDA} + aE_x^{HF} + b\Delta E_x^B + (1-c)E_c^{LYP} + cE_c^{LYP} \tag{3.11}$$

By using E_{xc} function, the Kohn-Sham (KS) equation can be solved by self-consistent method. At the first step, the electron density is defined. Then that electron density is used to solve KS equation for every electron in the system. The result is a new electron density value, and it used to solve KS equation. The iterative process is continue until the new electron density value is same with the previous value.

3.2 Møller-Plesset Perturbation Theory

Christian Møller and Milton S. Plesset described the Møller-Plesset Perturbation (MP) Theory in 1934 [29]. MP takes the zeroth-order Hamiltonian for an atom or molecule as the sum of the one particle Fock operator.

$$\hat{H}^0 = \sum_{i=1}^{N} \hat{F}(i) = \sum_{i=1}^{N} h(i) + V^{HF}(i) \tag{3.12}$$

We write the perturbation as the difference between the perturbed and unperturbed Hamiltonian

$$\hat{V} = \hat{H} - H^0 \tag{3.13}$$

The Hamiltonian is expressed as

$$\hat{H} = \sum_{i=1}^{N} f(i) + \sum_{i<j}^{N} g(i,j) \tag{3.14}$$

The Fock operator

$$\hat{F}(i) = \hat{f}(i) + V^{HF}(i) \tag{3.15}$$

The one electron operator, f in H and H are identical and can cancel each other in taking the difference in the perturbation

$$\hat{V} = \sum_{i<j}^{N} (r_{ij}^{-1} - V^{HF}) \tag{3.16}$$

The first-order correction the energy average of the perturbation over the unperturbed wavefunction can be described as:

$$E_0^{(1)} = \langle \psi_0 | \hat{V} | \psi_0 \rangle = \langle \psi_0 | (\frac{1}{r_{12}} - \hat{V}^{HF}) | \psi_0 \rangle \tag{3.17}$$

making the total first energy

$$E_n = E_n^0 + E_n^{(1)} = \sum_{a}^{N} \varepsilon_a - \frac{1}{2} \sum_{ab}^{N} \langle ab || ab \rangle \tag{3.18}$$

The energy throught first-order is simply Hartree-Fock energy.

The second-order MP, or MP2, is the most widely used method in quantum chemistry. The second-order correction to the ground state energy depends on the first order correction to the wavefunction. The first order wavefunction may be expanded as

$$\psi_{n0}^{(1)} = \sum_{a>b;r>s}^{N} C_{n,abrs}^{(1)} \psi_{ab}^{rs} \tag{3.19}$$

Where ψ_{ab}^{rs} respresent a wavefunction which has electron excited from spin orbital a and b (occupied) into spin orbital r and s (unoccupied), respectively. The coefficient C_{abrs} are determined by

$$C_{n,abrs}^{(1)} = \langle \psi_{ab}^{rs} | \psi_n^{(1)} \rangle = \sum_{a>b;r>s}^{N} \frac{\langle \psi_{ab}^{rs} | \psi_n^{(0)} \rangle}{\epsilon_a + \epsilon_b - \epsilon_r - \epsilon_s} \tag{3.20}$$

This wave function can be placed in the second order energy equation.

$$E_0^{(2)} = \sum_{a>b;r>s}^{N} \frac{\left| \langle \psi_0^{(0)} | \frac{1}{r_{12}} | \psi_{ab}^{rs} \rangle \right|^2}{\epsilon_a + \epsilon_b - \epsilon_r - \epsilon_s} \tag{3.21}$$

3.3 Hybrid Meta-generalized gradient-approximation (hybrid meta-GGA) exchange functional

The DFT fail for some kinds of systems, such as the polarizability of conjugated systems, and the ground-state energy of protonated polyenes. This failure contribute to the incorrect long-range behavior of the effective potentials generated by the density functional function. In order to correct the long-range error in DFT is by mixing the full Hartree-Fock correlation and the DFT correlation, the hybrid exchange-correlation energy, which can be written as equation (3.22).

$$E_{xc}^{hyb} = \frac{X}{100} E_x^{HF} + \left(1 - \frac{X}{100}\right) E_x^{DFT} + E_c^{DFT} \tag{3.22}$$

Where E_x^{HF} is the nonlocal Hartree-Fock exchange energy, X is the percentage of the HF exchange, E_x^{DFT} is the local DFT exchange energy, and E_c^{DFT} is the local DFT correlation energy.

The M06 functionals may be classified as hybrid meta-generalized gradient-approximations (hybrid meta-GGAs), which developed by Zhao and Truhlar [30, 31]. These functionals composed of four functional that have similar functional forms for the DFT part, but each parameter optimized to be used with a different percentage of HF exchange. The M06-2X has 54% HF exchange with a high nonlocality functional with double of the amount of nonlocal exchange (2X). This functional is good for all area in chemistry including thermochemistry and reaction kinetic, but excluding multireference system such as many systems containing transition metals.

The M06 and M06-2X functionals depend on three variables; spin density (ρ_σ), reduced spin density gradient (x_σ), and spin kinetic energy density (τ_σ).

$$x_\sigma = \frac{|\nabla\rho_\sigma|}{\rho_\sigma^{4/3}} \qquad \sigma = \alpha, \beta \tag{3.23}$$

$$\tau_\sigma = \frac{1}{2}\sum_i^{occup}|\nabla\Psi_{i\sigma}|^2 \tag{3.24}$$

The M06 functional form is a linear combination of the functional form of the M05, the first meta-GGA functional, and van Voorhis and Scuseria exchange correlation functional (VSXC) exchange functional is given by equation (3.25).

$$E_x^{M06} = \sum_\sigma \int dr\,[F_{x\sigma}^{PBE}(\rho_\sigma, \nabla\rho_\sigma)f(w_\sigma) + \varepsilon_{x\sigma}^{LSDA}h_X(x_\sigma, z_\sigma)] \tag{3.25}$$

where $F_{x\sigma}^{PBE}(\rho_\sigma, \nabla\rho_\sigma)$ is the exchange energy density of the Perdew-Burke-Ernzerhof (PBE) exchange model [32], $f(w_\sigma)$ is the spin kinetic energy density enhancement factor

$$f(w_\sigma) = \sum_{i=0}^{n} a_i w_\sigma^i \tag{3.26}$$

w_σ is a function of τ_σ, and $\tau_\sigma$is a function of the spin kinetic energy density τ_σ and spin density ρ_σ.

$$\omega_\sigma = \frac{(t_\sigma - 1)}{(t_\sigma + 1)} \tag{3.27}$$

$$t_\sigma = \frac{t_\sigma^{LSDA}}{t_\sigma} \tag{3.28}$$

$$t_\sigma^{LSDA} \equiv \frac{3}{10}(6\pi^2)^{2/3}\rho_\sigma^{5/3} \tag{3.29}$$

$\varepsilon_{x\sigma}^{LSDA}$ is the local spin kinetic energy density enhancement factor.

$$\varepsilon_{x\sigma}^{LSDA} = \frac{3}{2}\left(\frac{3}{4\pi}\right)^{1/3}\rho_\sigma^{4/3} \tag{3.30}$$

The last term on equation (3.25) is $h_X(x_\sigma, z_\sigma)$ which a Van Voorhis Scuseria exchange correlation potential is (VSXC), a kinetic energy density dependent exchange correlation functional [33]. These terms involve a working variable (z_σ) and two working function (γ and h) as described in equation (3.31).

$$h_X(x_\sigma, z_\sigma) = \left(\frac{d_0}{\gamma(x_\sigma, z_\sigma)} + \frac{d_1 x_\sigma^2 + d_2 z_\sigma}{\gamma_\sigma^2(x_\sigma, z_\sigma)} + \frac{d_3 x_\sigma^4 + d_4 x_\sigma^2 z_\sigma + d_5 z_\sigma^2}{\gamma_\sigma^3(x_\sigma, z_\sigma)}\right) \tag{3.31}$$

with

$$\gamma(x_\sigma, z_\sigma) = 1 + \alpha(x_\sigma^2 + z_\sigma) \tag{3.32}$$

$$z_\sigma = \frac{2\tau_\sigma}{\rho_\sigma^{5/3}} - C_F \tag{3.33}$$

$$C_F = \frac{3}{5}(6\pi^2)^{2/3} \tag{3.34}$$

In the M06-2X, the functional form of the exchange potential is $h_X(x_\sigma, z_\sigma)$ = 0.

Part II. The Properties of Carbonic Anhydrase

4 The π-stacking interaction between Trp5 and His64 on Human Carbonic Anhydrase II

4.1 Introduction

Aromatic ring, such as benzene, imidazole, indole, and phenol, have an additional stability caused by the arrangement of the π–electron above and below the plane of aromatic ring. These electrons caused π–electron cloud over the ring [34]. Four of 20 amino acids found in protein structures have aromatic ring, phenylalanine, tyrosine, tryptophan and histidine. The interactions that take place between the side chains of the aromatic amino acid residues are referred as aromatic–aromatic interactions. Aromatic residues are key of protein structures and have been shown to be important for structure stability, folding, protein-protein recognition, and ligand binding.

The Aromatic residues have a large internal rotation in their side chain. The $\chi 1$ angle (Cα-Cβ) and $\chi 2$ (Cβ-Cγ) rotation are restricted by packing their side chain into the tertiary structure of the protein, that confirmed by X-ray crystallography [13]. In Human Carbonic anhydrase II (HCAII), X-ray crystallography shows that histidine at position 64 have two conformation, “in” and “out” representing the direction of the ring toward and away from active site. The properties of imidazole chain of His64 are expected to tune by neighboring residues. Two of the closest residues with aromatic ring are Trp5 and Tyr7, which could trigger aromatic interaction with His64.

In this study, we determine the difference between “out” conformation and “in” conformation in the model system with Trp5 and/or Tyr7.

4.2 Computational Details

Three-model system was constructed to investigate the addition effect of Trp5 or Tyr7 to His64. The first model consists of three aromatic chains, Trp5, Tyr7 and “out” conformation of His64. We assemble these residues to make four structure; (A) His64, (B) Trp5-His64, (C) Tyr7-His64, and (D) Trp5-Tyr7-His64, as shown in

Figure 2. These structures were constructed using coordinate from X-ray coordinate file (Protein Data Bank (PDB) code: 2CBA). The hydrogen atom position rarely detected in X-ray crystallography, instead we artificially added hydrogen atom in our model structures. Considering two tautomeric form (Nδ1-H tautomer and Nε2-H tautomer) and imidazolium charged form, we constructed the structures for each form. Finally we have 12 structures for the “out” form of His64.

The Second model a structure was constructed in the same way of first model, but “out” conformation was replaced by “in” conformation. We constructed 12 structures for the “in” conformation of His64. In third model structure, we used benzene ring named Phe64, instead of using “out” conformation and “in” conformation of His64. Unlike imidazole, benzene does not have alternate form. We constructed 8 structures to replace “in” conformation and “out” conformation of His64. Totally we constructed 32 model structures.

We employed two calculation methods: (1) the DFT using Becke, three-parameter, Lee-Yang-Par (B3LYP) [26, 28] and second-order Møller-Plesset perturbation theory (MP2) [29]. The 6-31G(d,p) and 6-31++G(d,p) basis set was selected to our calculations. All calculation was performed under self-consistent reaction field (SCRF) method. All calculation was performed on NEC SX9 equipped with Gaussian 09 series of program [35].

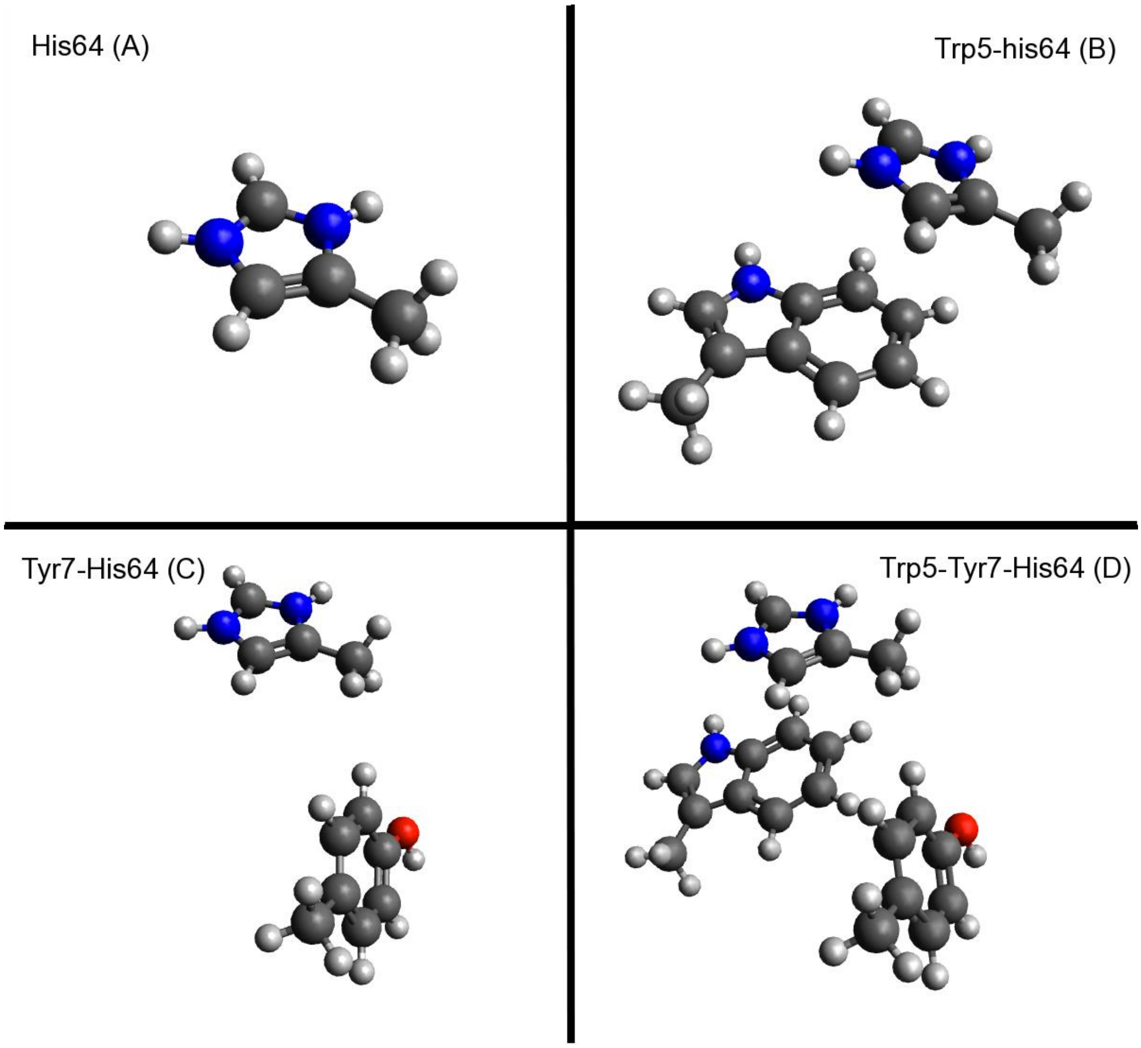
His64 (A)
Trp5-his64 (B)
Tyr7-His64 (C)
Trp5-Tyr7-His64 (D)

Figure 2. The constructed model structures to investigate the aromatic-aromatic interaction, which consist of the combination of Trp5, Tyr7, and His64

We employed two-step calculation. First, we optimize the hydrogen atoms in model structure using B3LYP/6-31G(d,p). During optimization, all hetero atoms (carbon, nitrogen, and oxygen) were fixed. Second, the energy of optimized structure was determine at higher levels of MP2/6-31G(d,p) and MP2/6-31++G(d,p). In order to compare with MP2/6-31++G(d,p), the B3LYP/6-31++G(d,p) also calculated. Finally we have four level of theory (B3LYP/6-31G(d,p)//(B3LYP/6-31G(d,p),

The energy of Nδ1-H tautomer and Nε2-H tautomer can be averaged, because the population of the Nδ1-H tautomer is known to be equal to the Nε-H tautomer [15]. We also assume the pH is equal to pKa, and then we can average the energy of imidazolium with the energy of neutral form. The energy of three forms of imidazole can be expressed by equation (4.1).

$$E = \frac{E_{im} + (E_{\partial 1} + E_{\varepsilon 2})/2}{2} \tag{4.1}$$

The difference energy between "in" conformation and "out" conformation can be expressed by

$$\Delta E = E_{in} - E_{out} \tag{4.2}$$

where E_{in} is the energy for model structure that have "in" conformation, and Eout is the energy for model structure that have "out" conformation.

4.3 Result and Discussion

4.3.1 Method and basis set comparison

Table 1 shows the energy data for each types of model structure and calculation level theory. We expected that the energy of DFT method is less accurate compared to MP2 method. In the MP2/6-31G(d,p)//B3LYP/6-31G(d,p) (can be simplified as

Table 1 ΔE for each model structure and calculation methods in kcal/mol

Method and Basis sets	A	B	C	D
B3LYP/6-31G(d,p)	0.50	0.22	1.21	0.78
B3LYP/6-311++G(d,p)	1.56	1.11	2.72	2.43
MP2/6-31G(d,p)	0.37	0.88	0.89	1.31
MP2/6-311++G(d,p)	0.36	2.09	0.94	2.60

MP2/6-31G(d,p) in Table 1), the ΔE value of structure A is 0.37 kcal/mol. When the indole ring of Trp5 was added to His64, the ΔE changed to 0.88 kcal/mol, i.e. structure B. The difference energy between structure A and structure B can be defined as energetic contribution of Trp5 to structure A, was 0.51 kcal/mol. By using the same method, we can estimate the energetic contribution of Tyr7 from structure C. The energetic contribution of Tyr7 was estimated to be 0.52 kcal/mol. Because the energetic contribution of Trp5 similar to Tyr7, we conclude that the π-stacking cannot be detected using this method. In the structure D, the energetic contribution of Trp5 and Tyr7 was 0.96 kcal/mol. So we decided to use a larger basis set, 6-31++G(d,p) to obtain the energy data.

By using a larger basis set, 6-311++G(d,p) combined with MP2, we obtain the DE for structure A is 0.36 kcal/mol. This value is similar to the value obtained from 6-31G(d,p) basis set. However, when the Trp5 added in structure A, the ΔE increased to 2.09 kcal/mol. The energetic contribution of Trp5 to His64 was 1.73 kcal/mol. the DE value for structure C was 0.94 kcal/mol, similar to the value obtained from 6-31G(d,p) basis set. The energetic contribution of Tyr7 was 0.56 kcal/mol. The energetic contribution of Trp5 and Tyr7 was added to ΔE of structure A to estimate the ΔE of structure D, by assuming that the interaction between Trp5 and Tyr7 was ignored. The predicted ΔE for structure D was 2.65 kcal/mol. In fact, this value is consistent with the calculated value from simulation, 2.60 kcal/mol. Based on this consistency, we suggest that the MP2/6-31++G(d,p)//B3LYP/6-31G(d,p) method was appropriate for determine π-stacking interaction.

4.3.2 Substitution of Imidazole with Benzene

In order to confirm our suggestion, we construct a similar structure to Figure 2 with replacing imidazole ring to benzene ring, namely Phe64, as shown in Figure 3. These structure was labeled as A’ to D’ structures. The comparison of ΔE between imidazole and benzene structure can be summarized in Table 2. Both structure calculated using the same method and basis set, MP2/6-31++G(d,p). The imidazole replacement to benzene causes a high decrease of ΔE in all structures. The ΔE of structure A’ and C’ were -1.34 kcal/mol and -1.40 kcal/mol, very low compared to other structures. The negative sign shows that each “in” conformation should be more stable than the “out” conformation. The addition of Trp5 to structure A’ increased the ΔE value to 0.52 kcal/mol. The energetic contribution of Trp5 was 1.86-kcal/mol. Use the similar method; the energetic contribution of Tyr7 to structure A was -0.06 kcal/mol. Then the predicted ΔE of structure D’, obtained by adding energetic contribution of Trp5 and Tyr7 to ΔE of structure A, was 0.46 kcal/mol. This value was consistent with the ΔE value obtained from calculation 0.50 kcal/mol. The energetic contribution of Trp5 to His64 and Phe64 was estimated to be almost same, 1.73 kcal/mol and 1.83 kcal/mol, respectively. We conclude that the energy of π-stacking effect of Trp5 was between 1.73 and 1.83 kcal/mol to stabilize the “out” conformation of HCAII, compared to “in” conformation.

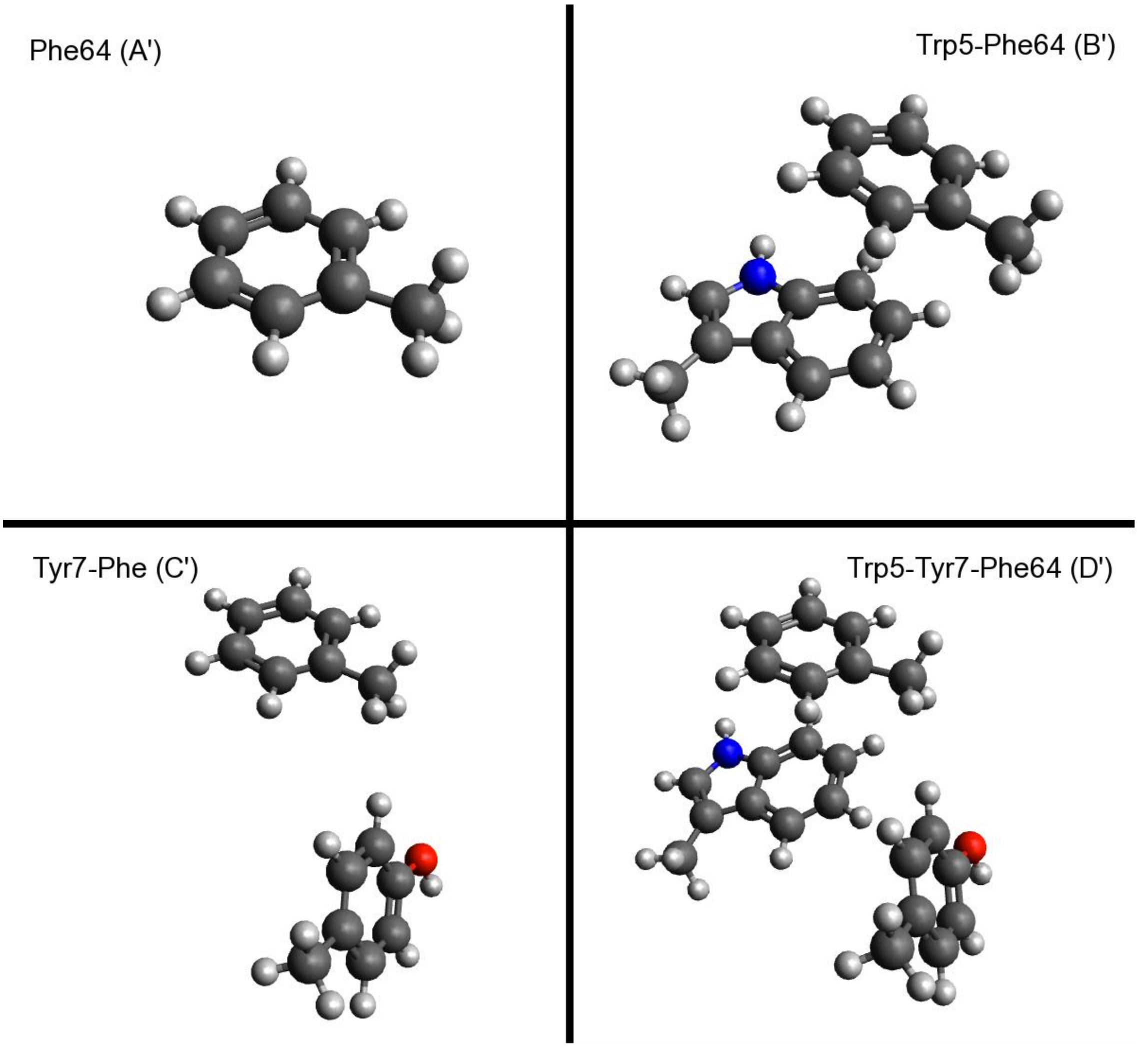
Phe64 (A')
Trp5-Phe64 (B')
Tyr7-Phe (C')
Trp5-Tyr7-Phe64 (D')

Figure 3. The constructed model structure, where His64 was substituted with Phe64.

Table 2 ΔE energy comparison between imidazole (His) and benzene (Phe) in kcal/mol

Structure	ΔE	Structure	ΔE
A	0.36	A’	-1.34
B	2.09	B’	0.52
C	0.94	C’	-1.40
D	2.60	D’	0.50

4.4 Conclusions

We have analyzed the π-stacking interaction caused by Trp5 to two conformations of His64 that can be seen in crystal structure of HCAII. Geometry optimization was performed using DFT method and medium level of basis set (B3LYP/6-31G(d,p)). The energy calculation including π-stacking interaction was best suited estimated with (MP2/6-31++G(d,p)). The π-stacking interaction was occurred in the “out” conformation, by the value between 1.73-1.83 kcal/mol.

From these results, we should consider the properties of Trp5 in the calculation that include the active site of HCAII. We cannot ignore the π-stacking interaction between Trp5 and the “out” conformation of His64.

5 Tautomeric forms of His64 and The Difference Energies

5.1 Introduction

Among 20 naturally amino acids, Histidine is a unique residue. More than 50% of all enzymes use at least one Histidine in their active sites. This probably caused by of high versatility of its imidazole rings. Imidazole ring has two neutral forms (Nδ1-H and Nε-2 H tautomer) and a protonated form (imidazolium ion), with one form favored over the other by the protein environment and pH. The pKa value of Histidine is 6.6, around neutral pH, allowing the deprotonated nitrogen of its imidazole ring as an effective ligand for metal binding. It also has been suggested that tautomerization and variation of χ1 angle of His are crucial part of the proton-transfer process.

Human Carbonic Anhydrase II (HCAII). HCAII is a zinc-metalloenzyme that catalyzes the CO_2 to HCO_3^-. X-ray crystallography data shows that His64 have two alternate position, designated as “in” conformation and “out” conformation, representing the direction of imidazole ring toward and away from active site [13]. These two conformations of His64 has been assumed to be connected with the final step of proton transfer. A molecular dynamics simulation has been reported to explain this relation [36]. However the Trp5, that give a π-stacking interaction with His64, was not included in the model system. Here we calculate the interaction between His64 and Trp5 in the relation of χ1 angle rotation on two neutral form and protonated form of His64 of HCAII. The χ1 angle is an angle that designated of N-

Cα-Cβ-Cγ angle, in short Cα-Cβ angle, of Histidine. We calculate the energy profile of χ1 rotation through “in” conformation and “out” conformation.

5.2 Computational Details

Two model structures were constructed to investigate the difference energy caused by the addition of Trp5 on His64. The first model structure (Model A) consists of the four residues, Trp5, Gly63, the “out” conformation of His64, and Ala65. The second model structure (Model B) consist the same residues as Model A but without Trp5 residue. The coordinates were obtained from the X-ray coordinate file (Protein Database Bank (PDB) code: 2CBA). The hydrogen atoms were artificially added in both model structures. By considering two neutral form and protonated form of His64, we constructed three types of structure, Nδ1-H tautomer, Nε2-H tautomer and imidazolium ion form. In order to obtain an energy profile, twelve points of χ1 angle (-98.6°, -78.6°, -58.6°, -38.6°, -18.8°, -10°, 1.4°, 10°, 21.4°, 41.4°, 61.4°, 81.4°, and 101.4°) were manually adjusted for each types of structure. We have 36 structures for each Model A and Model B, totally 76 model structures were constructed.

The geometry optimization was performed to determine the position of hydrogen atoms in all model structure, by the B3LYP method [26, 28]. During optimization, all heteroatoms were fixed. The B3LYP is good enough for geometry optimization. However, we are considering the interaction between electrons, such as π-stacking interaction, it is necessary to use a theory that include electron correlation. The second order Møller-Plesset Perturbation theory (MP2) was used to determine the energy of a structure that already optimized using B3LYP method [29]. Self-consistent reaction field (SCRF) method were used on all calculation (ε=4.24).

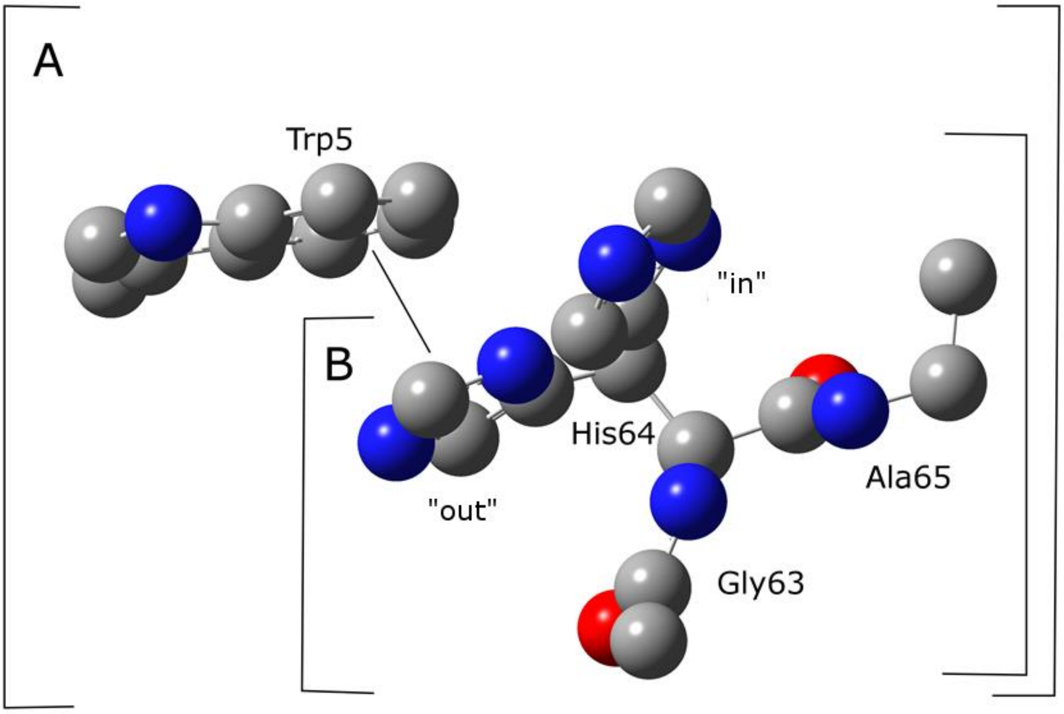
A
Trp5
"in"
B
His64
Ala65
"out"
Gly63

Figure 4. A) A Model system of Trp5-Gly63-His64-Ala65 structure. B) B Model A is Gly63-His64-Ala65 structure. The χ1 angle was rotated to obtain the energy profiles in both model structures.

5.3 Results and Discussion

5.3.1 The Energy Profile of B3LYP Method

Figure 5 shows plot of the calculated energy value for each types of imidazole forms. The x-axis represents the $\chi 1$ angle, while the y-axis represent the energy in kcal/mol. In order to compare Model A and Model B, we superimposed two curves of energy data. The π-stacking interaction was expected to occur in “out” conformation or negative region of $\chi 1$ angle, because the His64 form planar parallel with Trp5. We also expect at “in” conformation or the positive region of $\chi 1$, the π-stacking interaction getting weaker or no π-stacking interaction. By using this assumption, we superimposed the energy profile of Model A and Model B at the highest $\chi 1$ angle (101.4°). Then we set the lowest energy value of each type of imidazole to 0. Then set other energies value become relative to the lowest one.

Figure 5A, B, and C shows the energy profiles for Nδ1-H tautomer, Nε2-H tautomer and protonated form, respectively, using B3LYP method. The closed circle line represents the energies data of Model A, while the open circle for the energies data of Model B. There are characteristically double-well potential in all profiles. The two potential well exist in positive (“in”) and negative (“out”) region of x-axis. The addition of Trp5 to His64 model structure (Model B) was increasing the stabilization energy of “out” conformations in neutral form, while in protonated form is no different between both of them. In Nδ1-H tautomer, the “in” conformation was more stable compared to “out” conformation. Another two forms, Nε2-H tautomer and protonated form, shows a different behavior compared to Nδ1-H tautomer, the “out” conformation is more stable compared to “in” conformation. To clearly see these the

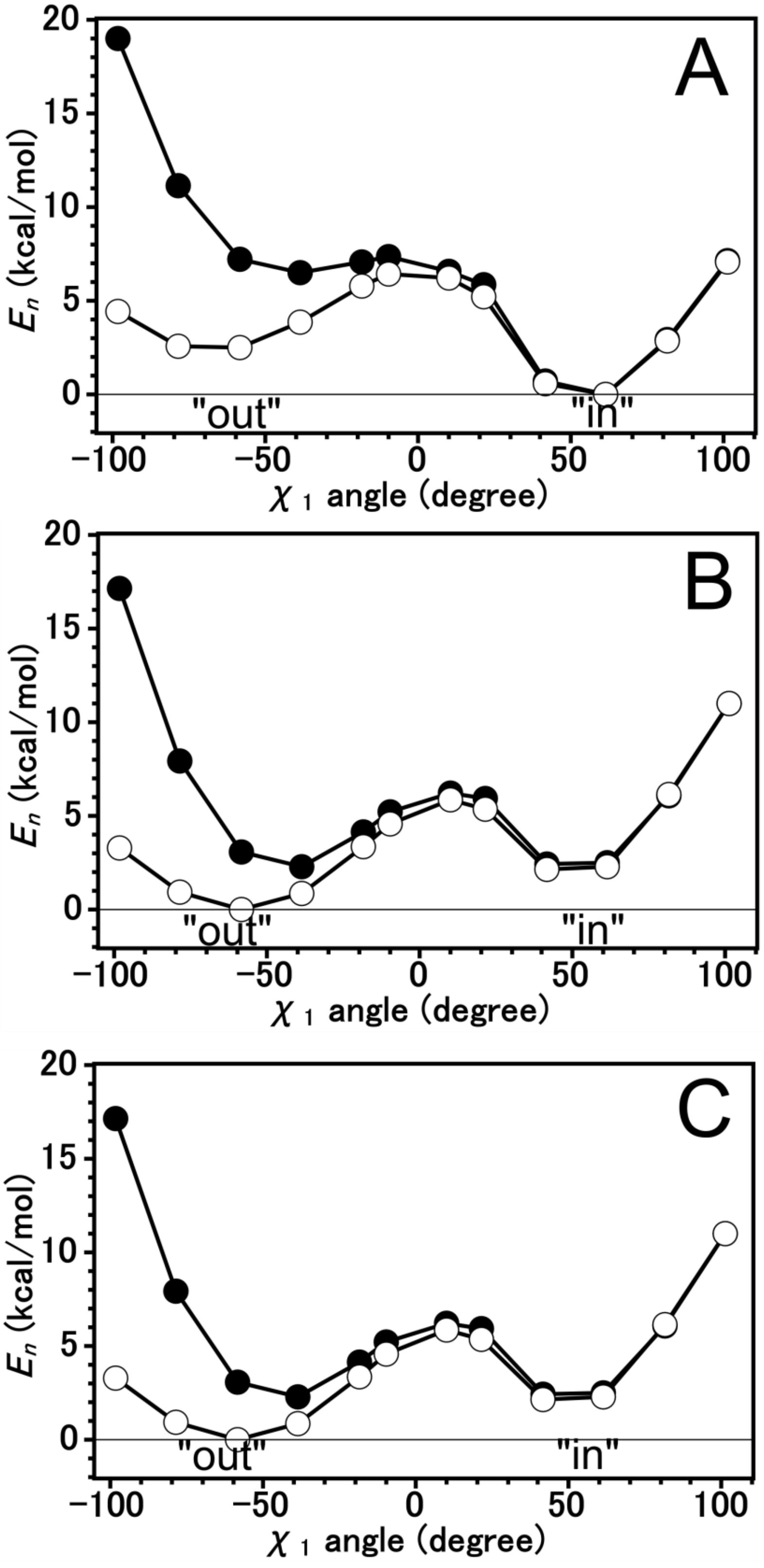

Figure 5. The energy profile curves of His64 rotation within Model A and Model B using B3LYP method. The closed circle along the solid line refer to Model A, and the open circle along the solid line refer to Model B. A) Refer to Nδ1-H tautomer, B) refer to Nε2-H tautomer, and C) refer to protonated form.

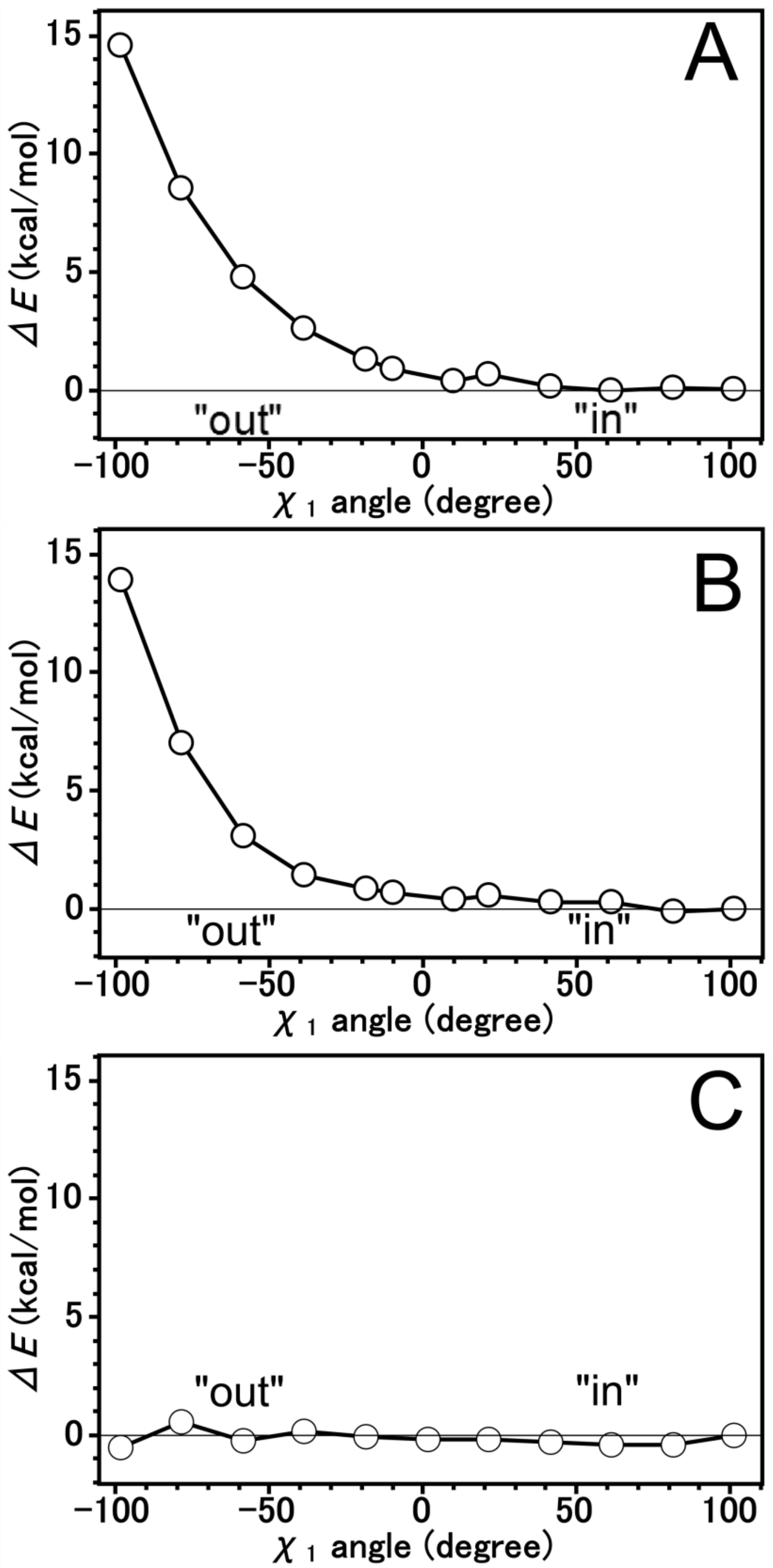

Figure 6. The energy difference between Model A and Model B for Nδ1-H tautomer (A), Nε2-H tautomer (B), and protonated form (C) using B3LYP method.

comparison between Model A and Model B, we plot the difference energy between them as a function of χ1 angle, as shown in Figure 6. The difference energy of Nδ1-H tautomer and Nε2-H tautomer seem to be similar with the energy difference has high value at the most negative χ1 angle and decreased in the positive way of the χ1 angle. The protonated form shows a different behavior, in which the energy difference seems stable in all χ1 angles.

5.3.2 The Energy Profile using MP2 method

As mention in previous section, B3LYP is not a good method to determine electronic interaction. The MP2 method is a better way to determine the electronic interaction. Figure 7 shows the MP2 plot for all three types of imidazole forms. It shown in all plot that the energy profile of Model A was lower than Model B in "out" region, indicating that the indole of Trp5 interact with imidazole of His64 to stabilize the structure. Figure 7A shows the energy profile for Nδ1-H tautomer. The "in" conformation was more stable compared to "out" conformation by 4.5 kcal/mole for Model A and 3.6 kcal/mole for Model B. It different with the Nε2-H tautomer and protonated form, the "out" conformation was more stable compared to the "in" conformation. Nε2-H tautomer "out" conformation for Model A and Model B was more stable compared to "in" conformation by 4.2 kcal/mole and 1.2 kcal/mole respectively, as shown in Figure 7B. While in protonated form, the "out" was more stable than "in" conformation by 6.9 kcal/mole for Model A and 2.9 kcal/mole for Model B, as shown in Figure 7C. Figure 8 shows the energy difference between Model A and Model B using MP2 method. At the "out" region, a potential energy well can be seen. B3LYP method did not give this kind of results. These stabilization are probably occur because of the π-stacking interaction between Trp5 and the "out"

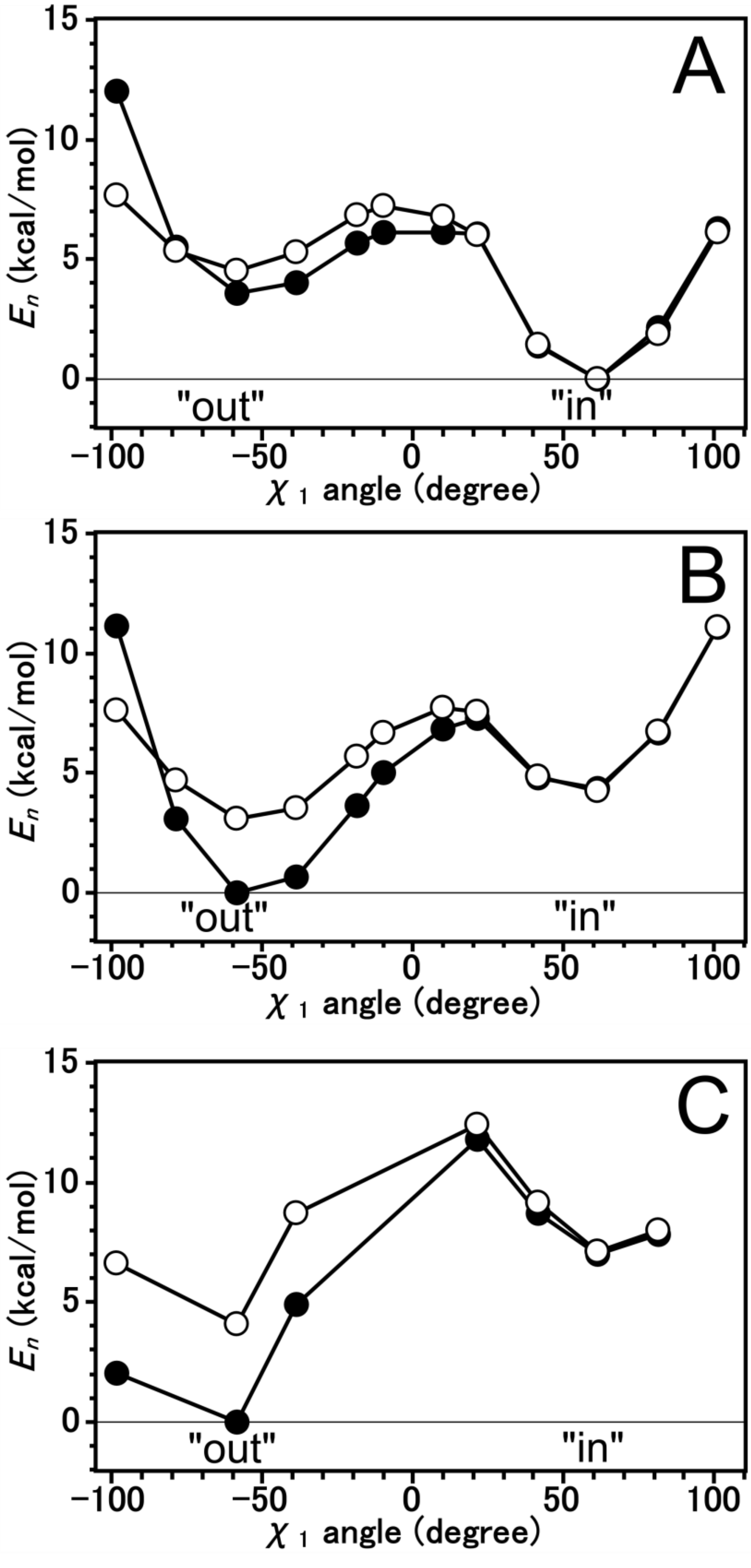

Figure 7. The energy profile curves of His64 rotation within Model A and Model B using B3LYP method. The closed circle along the solid line refer to Model A, and the open circle along the solid line refer to Model B. A) Refer to Nδ1-H tautomer, B) refer to Nε2-H tautomer, and C) refer to protonated form.

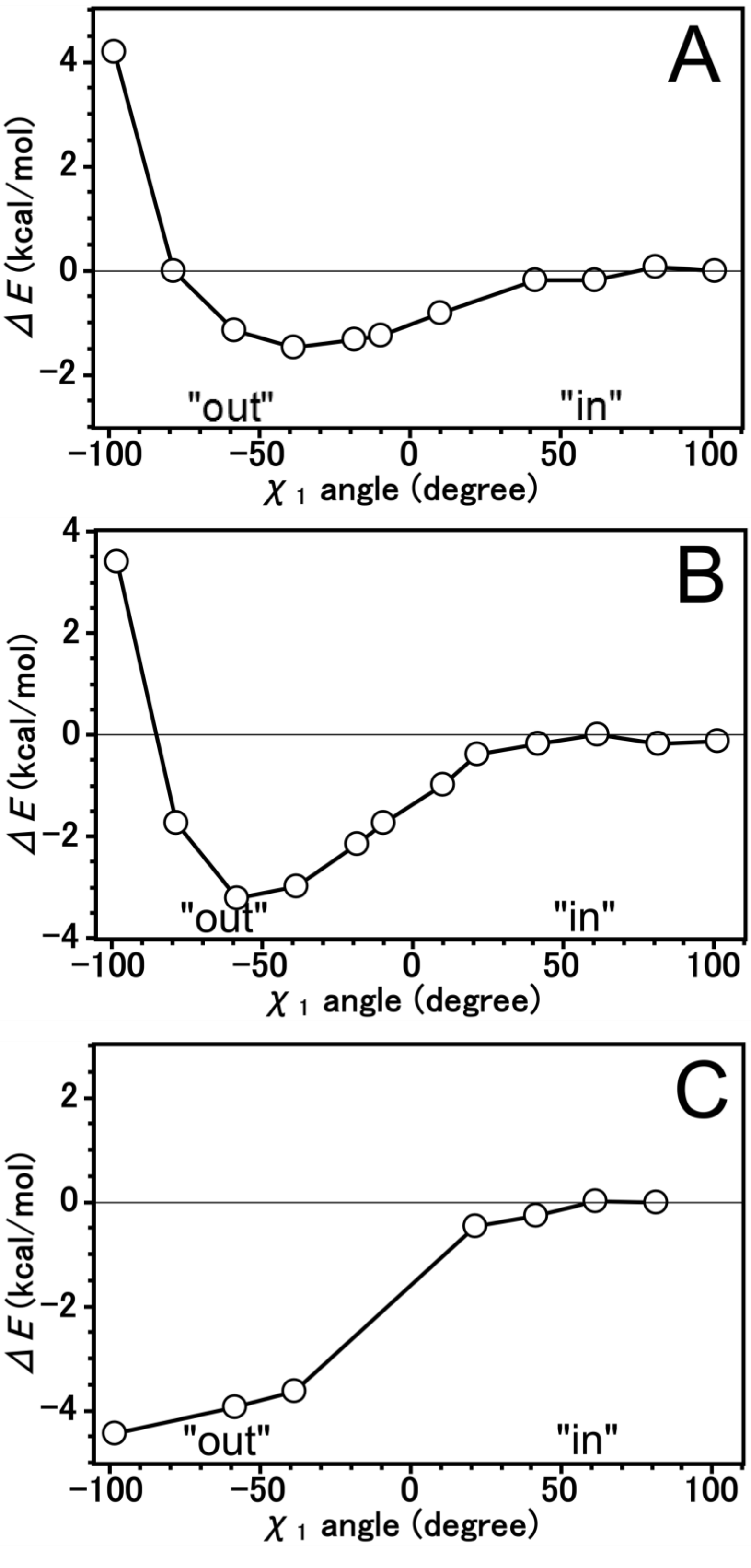

Figure 8. The energy difference between Model A and Model B for Nδ1-H tautomer (A), Nε2-H tautomer (B), and protonated form (C) using MP2 method.

conformation of His64.

5.4 Conclusion

The π-stacking interaction cannot be ignored in determine the potential energies when there is a rings in model structure. The π-stacking interaction is poorly detected by B3LYP method. On the other hands, the MP2 method offers a better result when there is a π-stacking interaction. In our model structure we observe this interaction in two tautomeric forms and a protonated form of His64. In all forms, the structure at "out" conformation become more stable, that resulting the height of the potential barrier increased. This suggests that explaining the transfer of proton using rotational motion is not appropriate.

6 Interaction energy of Trp5 to Tautomeric forms and imidazolium ion of His64

6.1 Computational Details

Binding energy is an amount of energy required to separate a particle from a system of particles. I general binding energy of molecule A to molecule B can be written as equation (6.1).

$$\Delta E_i = E_{AB} - (E_A + E_B) \tag{6.1}$$

Similar with Figure 4, the model structure consists of Trp5, Gly63, “out” conformation of His64, and Ala65 of HCAII to construct our model structure. To obtain the binding interaction energy profile, we need an energy of a model structure consist only Trp5, we construct three model structure, as shown in Figure 9. The first model structure, Model A, consist of Trp5 residue. The second model structure, or Model B, consist of Gly63, “out” conformation of His64, and Ala65 residues. The combination of Model A and Model B was the third model structure, Model AB. The model structures were constructed using the coordinates obtained from the protein database bank (PDB) of 2CBA. The $\chi 1$ angle of His64 was manually rotated to obtain the energy profile. The hydrogen atoms were added to all model structures by considering two neutral forms and one protonated form of His64. We calculate the energy profile for each of His64 forms. We perform two-step calculation, optimization and energy calculations. The M06-2X, a new hybrid meta-exchange correlation functional, constructed by Zhao and Truhlar were employed to optimize the position of hydrogen atoms [30, 31]. The M06 family is a better method

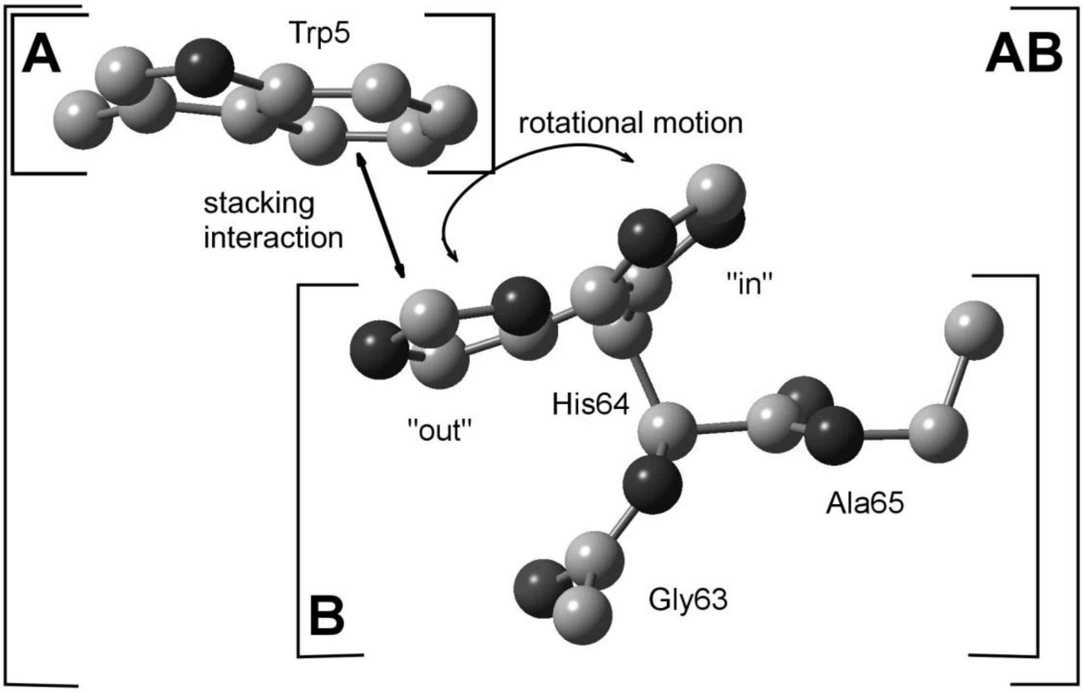
A
Trp5
AB
rotational motion
stacking
interaction
"in"
"out"
His64
Ala65
Gly63
B

Figure 9. Three model structure constructed. A. Trp5, B. Gly63, His64, and Ala65, AB) the combination of model structure A and B.

compared to B3LYP for main group thermochemistry, thermochemical kinetics, noncovalent interaction, excited states, and transition elements. Note that all heteroatoms were fixed during optimization. After optimizing the hydrogen position of Model AB, we divide it to Model A and Model B, as shown in Figure 9. Single point energy calculations under M06-2X were performed for Model A and Model B to obtain the interaction energy profile for M06-2X method [29]. In order to obtain the interaction energy profiles, single point energy calculation under MP2 also performed for Model AB, Model A, and Model B.

In studies that related to weakly bound cluster, the basis set superposition error could occur [37, 38]. Counterpoise method is prescription for removing the BSSE. For interaction between model A and model B, the uncorrected interaction energy would be computed as equation (6.2):

$$E_{int}(AB) = E_{AB}^{AB}(AB) - E_{A}^{A}(A) - E_{B}^{B}(B) \tag{6.2}$$

However the counterpoise method could not easily combined with SCRF method. We did not consider the BSSE, because the condition for this simulation is supposed to be in the ether condition (ε=4.24).

6.2 Results and Discussion

6.2.1 M06-2X calculation

Figure 10 shows the energy profile of Model AB and Model B by using M06-2X method. Energies of Model AB represented by closed circle and the open circle represent the energies of Model B. We superimposed both curves in the “in” region. The energy profiles of M06-2X give a better π-stacking interaction result; the energies of Model AB at “out” region tend to decrease, compared than B3LYP

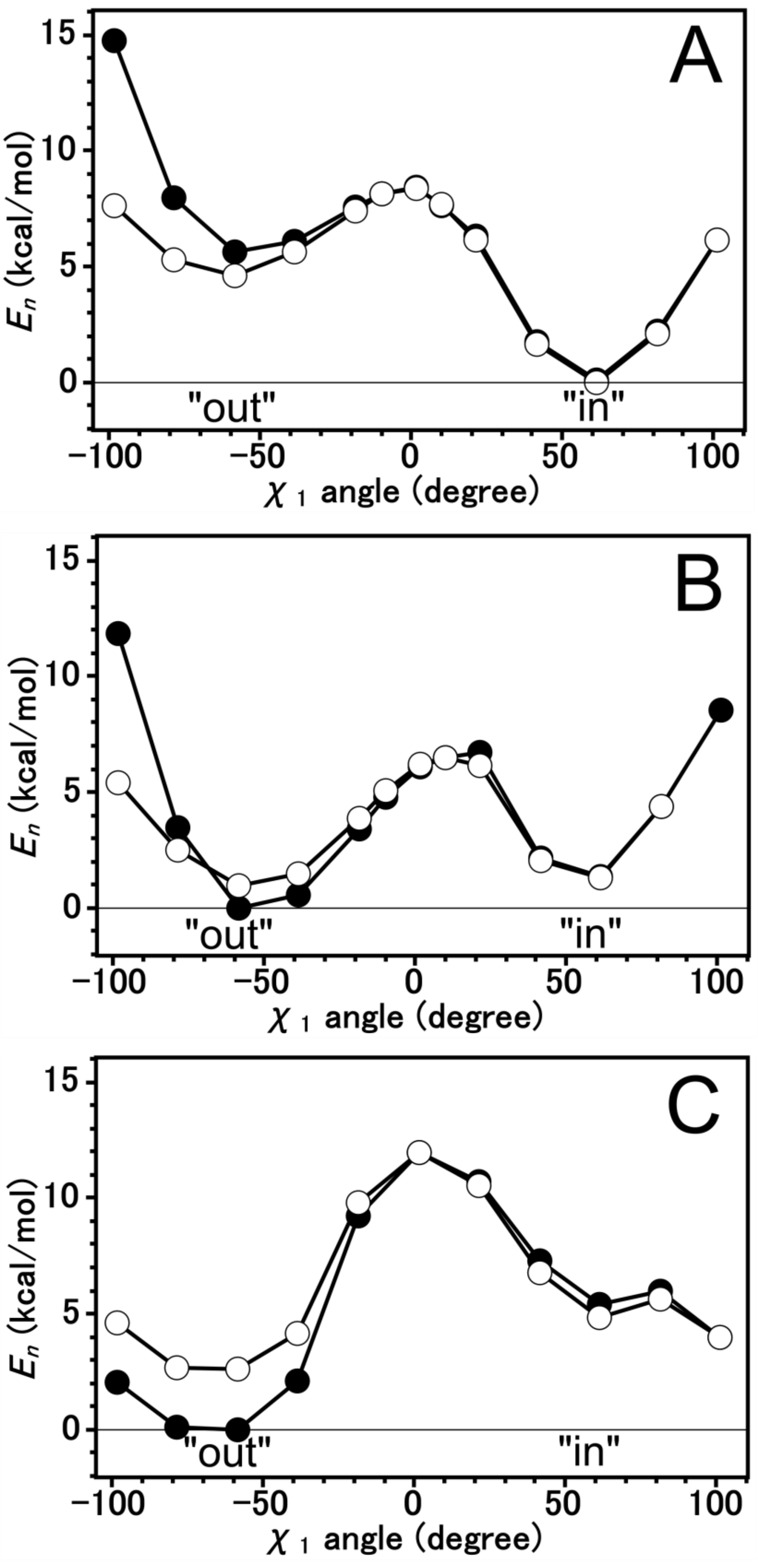

Figure 10. The energy profile curves of His64 rotation within Model A and Model B using M06-2X method. The closed circle along the solid line refer to Model A, and the open circle along the solid line refer to Model B. A) Refer to Nδ1-H tautomer, B) refer to Nε2-H tautomer, and C) refer to protonated form.

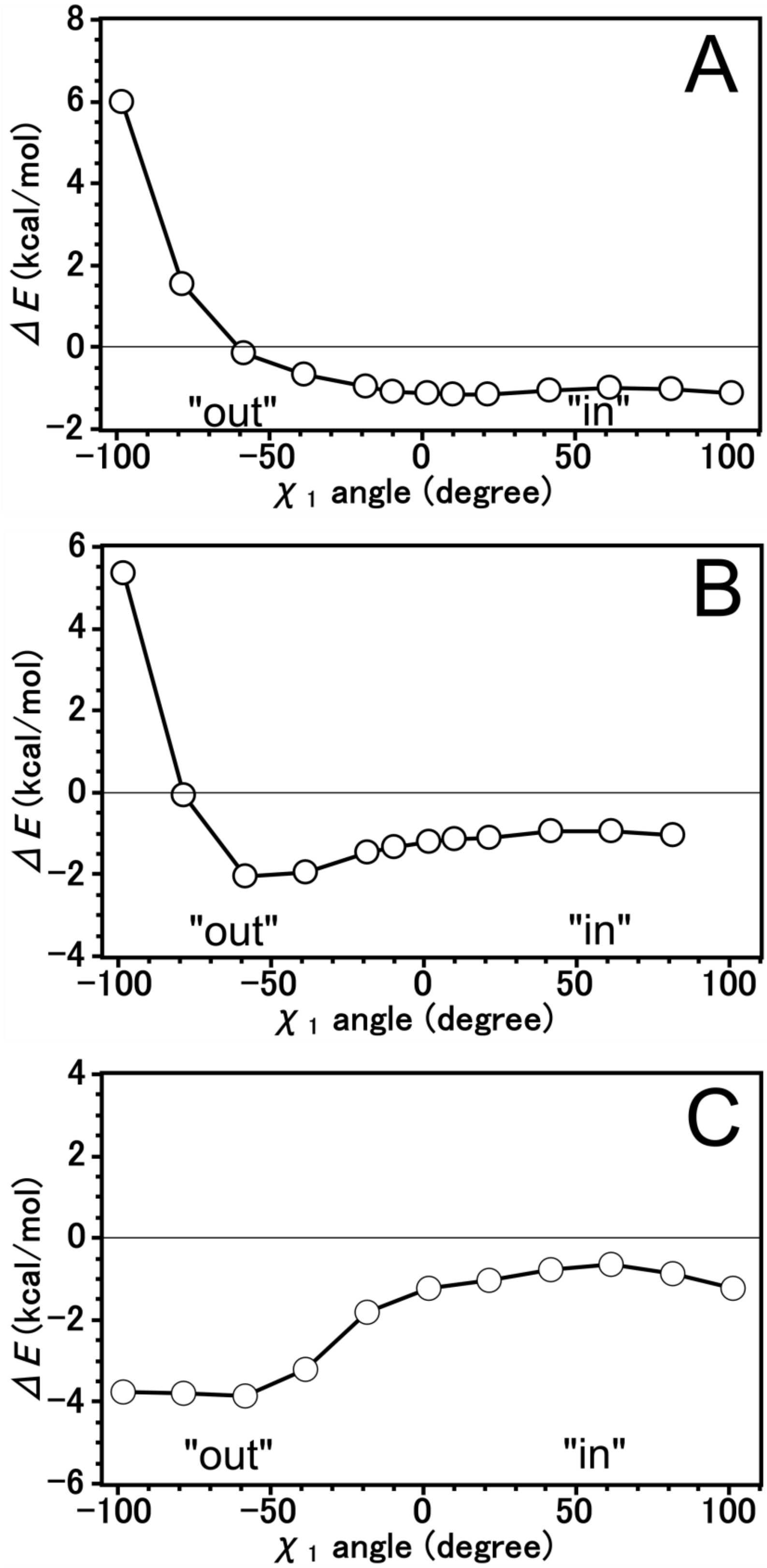

Figure 11. The interaction energy profile of A) Nδ1-H tautomer, B) Nε2-H tautomer, and C) protonated form using M06-2X method.

results. The energies of Model AB at “out” region are lower than Model B, except for Nδ1-H tautomer. In this section we calculate the binding interaction energy by using equation (6.1). In binding interaction energy, we consider the Trp5 as a single model structure. The binding interaction energy is more appropriate than difference energy between Model A and Model B. We got the real value of binding energy, instead set the lowest energy value to zero as the difference energy. Figure 11 shows the interaction energy profile by M06-2X method. Small decreases at the “out” region indicate that the M06-2X method can detect the π-stacking interaction.

6.2.2 MP2 calculation

The M06-2X is a good method for calculates medium range interaction. However the MP2 method theoretically give a better result for energy calculation. The optimization process of B3LYP and M06-2X were compared using single point calculation of MP2 method. Figure 12 shows the potential energy curve of MP2 using the optimized structure of M06-2X. The plot is similar to the plot of MP2 using the optimized structure of B3LYP method, shown in Figure 7.

Figure 13 shows the interaction energy profile using MP2 method. Compared to difference energy, the interaction energy gives an exact value rather than set the lowest energy relative to zero. The shape of curves are similar to the interaction energy curves, Figure 8.

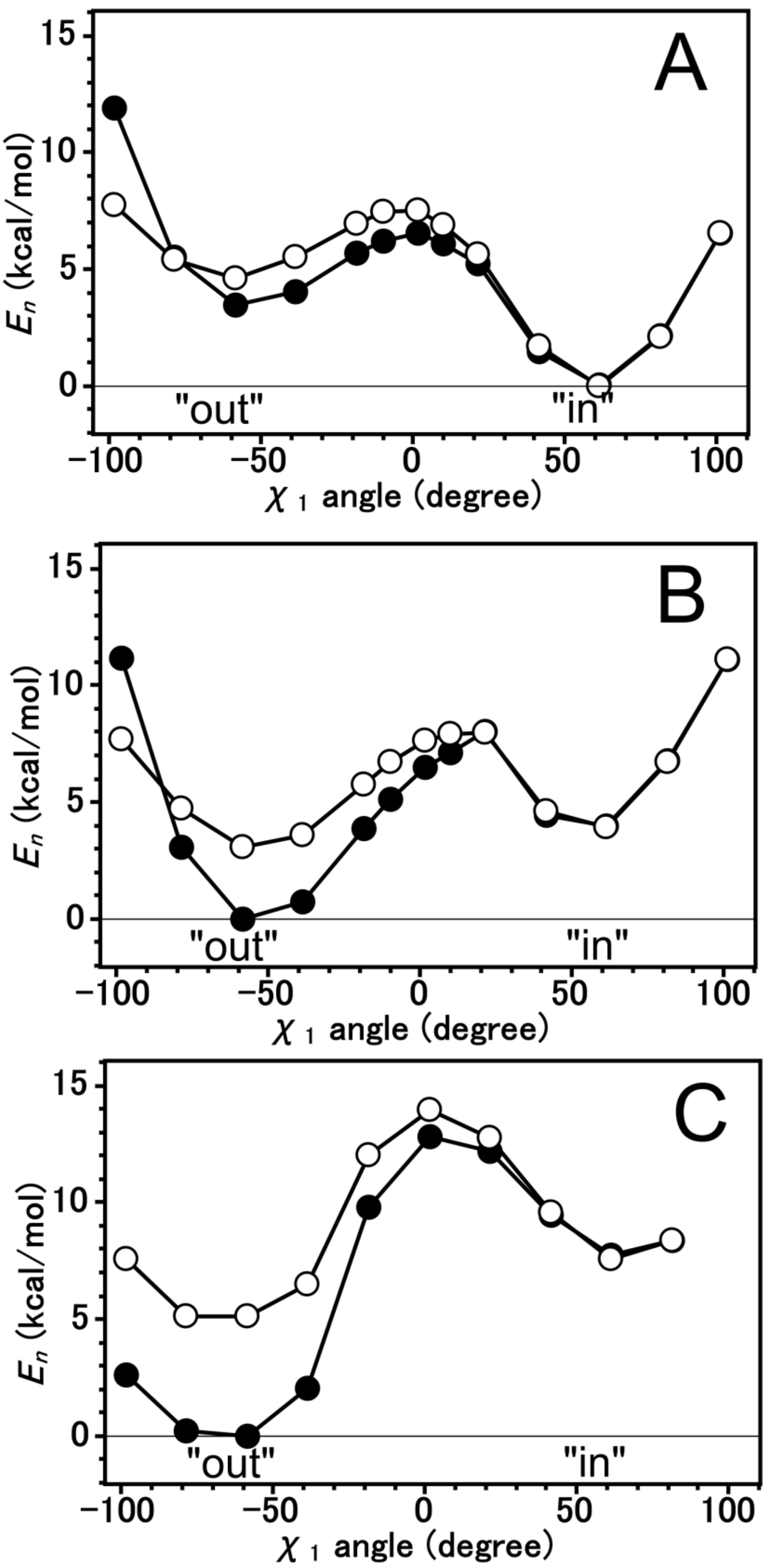

Figure 12. The potential energy profile of MP2 using the obtained structure of M06-2X. A) Refer to Nδ1-H tautomer, B) refer to Nε2-H tautomer, and C) refer to protonated form.

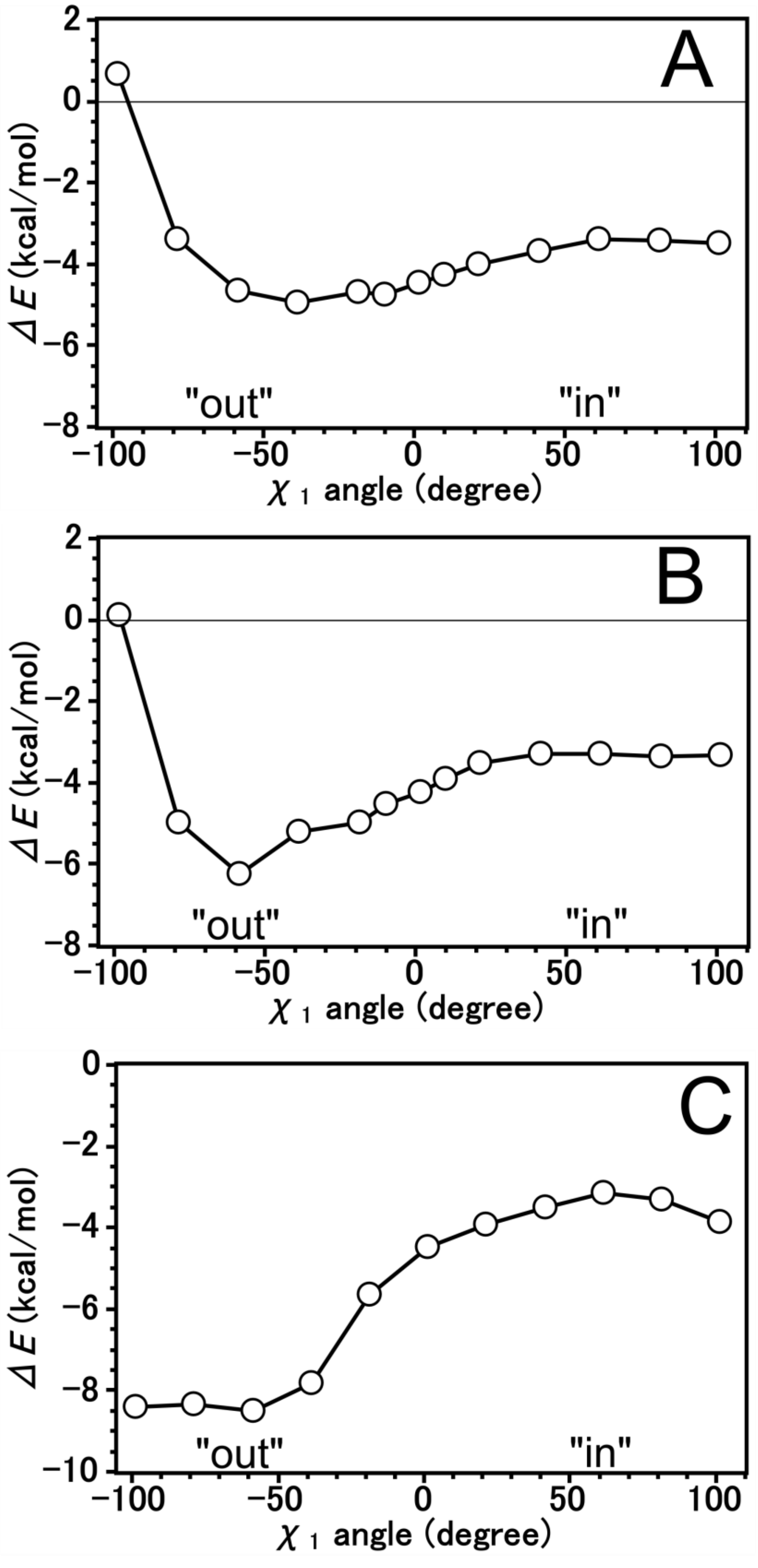

Figure 13. The interaction energy profile of MP2 calculation. A) refer to Nδ1-H tautomer, B) refer to Nε2-H tautomer, and C) refer to protonated form.

6.3 Conclusion

We have investigated the optimization results using M06-2X method, using the same structure as the previous chapter. The M06-2X and B3LYP provided similar result in the geometry optimization. However in energy calculation, the M06-2X provide more reliable results. M06-2X included the medium range interaction, such as π-stacking interaction. Due to similar optimization result, the interaction energy profile shows the similar curve with the difference energy. The difference between them is the interaction energy obtains the exact value of energy, while the difference energy is relative (manually set the lowest energy to zero).

Part III. General Conclusions

7 General Conclusion

7.1 The π-stacking interaction to His64

The Trp5 residues induce the π-stacking interaction with the "out" conformation of His64. This interaction is contribute to the stabilization energy, and should be considered in explaining the mechanism of HCAII. The (MP2/6-31++G(d,p) calculation level was good enough to determine this interaction. The calculated energetic contribution for Trp5 to His64 or π-stacking interaction was 1.73~1.83 kcal/mol.

7.2 Potential Energy Profile

The potential energy profiles of the rotation at $\chi 1$ angle are found to be dependent with the tautomeric forms of His64. The Nδ1-H tautomer prefers the "in" conformation, while the other two forms (Nε2-H tautomer and protonated form) prefer the "out" conformation. The π-stacking interactions make the potential well at the "out" region become deeper. The deep of potential wells related to the energy barrier between two potential wells needs to be considered for explaining the mechanism the transfer of proton by the rotational of motion. The value of barrier varies from 6 to 10 kcal/mol. These values indicate that π-stacking interaction would restrict the rotational motion of the imidazole ring of His64.

7.3 The Interaction Energy Profile

The optimization results of M06-2X method give the same geometry as B3LYP, but the calculated energy was better, because the medium range interaction also included.

The binding interaction energy of the His64 rotation has been estimated by MP2 method. At “out” region, the π-stacking interaction induces the stabilization of the model structures. The protonated form has highest stabilization compared to the two tautomeric forms.

7.4 Future works

In the thesis, the B3LYP, M06-2X and MP2 method have been used to investigate the structural and energetic properties of small model structure of HCAII. We are focusing on the tautomeric form and protonated form of His64. In the next step, more comprehensive study of structural properties of HCAII will be investigated. Furthermore more complex structure, including the zinc atom and hydrogen bonding-bridge between His64 and zinc atom should be considered. Perhaps, it could help explaining the process of transfer of proton.

.

Appendix

Appendix A. Approaching Proton Relay in Human Carbonic Anhydrase II

A.1 Introduction

HCAII have zinc ion in the active site. The zinc atom bound with a water molecule to form a zinc-bound water. This zinc-bound water construct a tetrahedral complex with three histidine residues, His94, His96, and His119.

In the active site of HCAII, several oxygen atoms of water molecules are located between zinc atom and His64 residue [13]. These water molecules form a hydrogen bond bride that connected the zinc-bound water and the imidazole ring of His64. His64 is accepted to facilitate the transfer of proton from zinc-bound solvent to buffer molecule. The pH-dependent X-ray crystallography shows that His64 has two conformations, “in” and “out”. At acidic pH, His64 prefer the “out” conformation, which the imidazole ring is planar parallel with the indole ring of Trp5. The Hi64 prefer the “in” conformation in the base condition [39].

NMR studies of His64 in HCAII suggest that the proton-transfer process is associated with the tautomerization of His64 [15]. At the neutral pH, the nitrogen atoms of imidazole ring serve as donor and acceptor. Decreasing the pH, caused the conformation change. The detail can be seen in Figure 14.

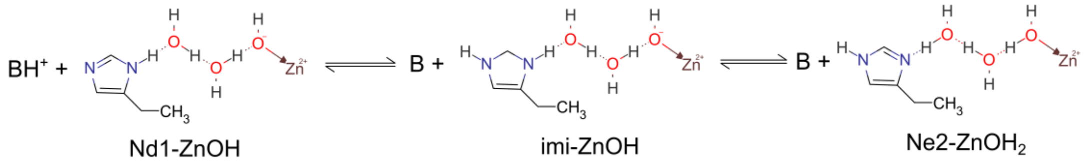

Figure 14. Conformational profiles of His64 linking with zinc atom *via* hydrogen bond network.

A.2 Computational Details

The model structure was constructed using the coordinate of PDB file (code: 2CBA). Due to the limitation of computer capabilities, the calculation did not performed on the whole protein. We selectively extracted the active site residues (Trp5, Tyr7, Gly63, His64, Ala65, Asn67, His94, His96, His119, and Thr200), zinc ion, and four oxygen atoms of water molecules (ZnO, w1a, w2, and w3a), as shown in Figure 15. Hydrogen atoms were artificially added into structure. Considering four types of histidine, that shown in Figure 14, we construct a model structure for each types. For these structures, the $\chi 1$ angle of His64 were manually rotated from -98.4° to 101.6° by 3~20 degree. Totally we have constructed almost 72 model structures.

The M06-2X method was employed to obtain the optimized geometry of all model structures [30, 31]. In order to obtain energy data, the second order Møller-Plesset perturbation theory (MP2) [4] was performed on the optimized structures. All calculation was combined with the 6-31G(d,p) basis set, and self-consistent reaction field (SCRF) method. In order to give the hydrophobic environment in protein, diethyl ether was selected as a solvent ($\varepsilon = 4.24$). The high performance and large-scale memory machine, SGI Altix UV 100, equipped with Gaussian 09 series of program was used in all calculations [35].

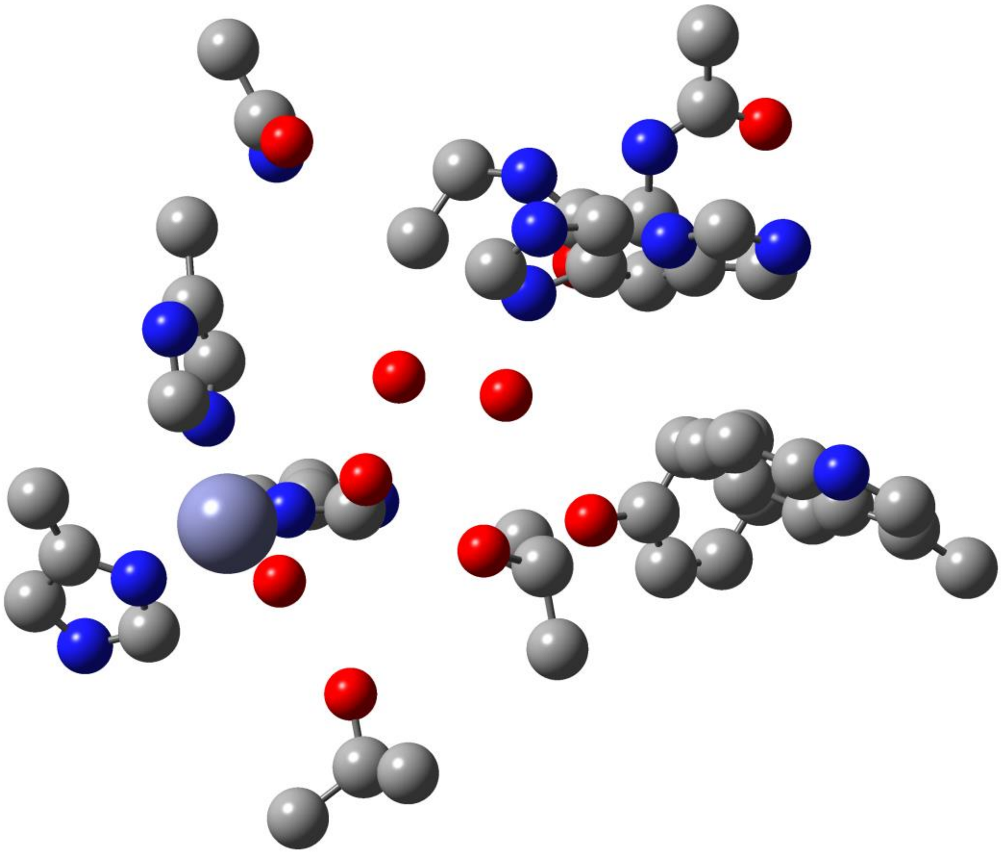

Figure 15. The constructed model structure, consist of zinc atom, four water molecules and surrounding residues (Trp5, Gly63, His64, Ala65,

A.3 Results and Discussion

A.3.1 Geometry Optimization

Geometry optimization on such a large model structures was not easy. In order to save resources and time, we divide the optimization process into three steps. The schematic process of optimization can be seen in Figure 16. First, the model structure was divided into two group: g1 and g2. The g1 is a model structure without three oxygen atoms (w1a, w2, and w3a), and remain the AS residues, zinc ion, and ZnO. Then position of hydrogen atoms in all g1 structure was optimized under M06-2X method.

The g2 structure consists of three remaining water molecules (w1a, w2, w3a). These atoms were returned to the optimized structure of g1, called g1g2 structure. The optimized structures of g1 that has the $\chi 1$ angle more than 60° were abandoned because the w2 oxygen atoms overlapped with the $\varepsilon 1$-hydrogen of His64. For the remaining structure, the hydrogen atoms were added to three oxygen atoms (w1a, w2, and w3) by considering the tautomerization and pH as shown in Figure 14. The position of hydrogen atoms we adjusted to make a possible hydrogen bond bridge as shown in Figure 15. Then we performed the second optimization for hydrogen atom in w1a, w2, and w3a water molecules by fixing the coordinates of another atoms. In order to confirm the optimization, we perform the last optimization of hydrogen atoms fixing coordinates of all heteroatoms for g1g2 structure.

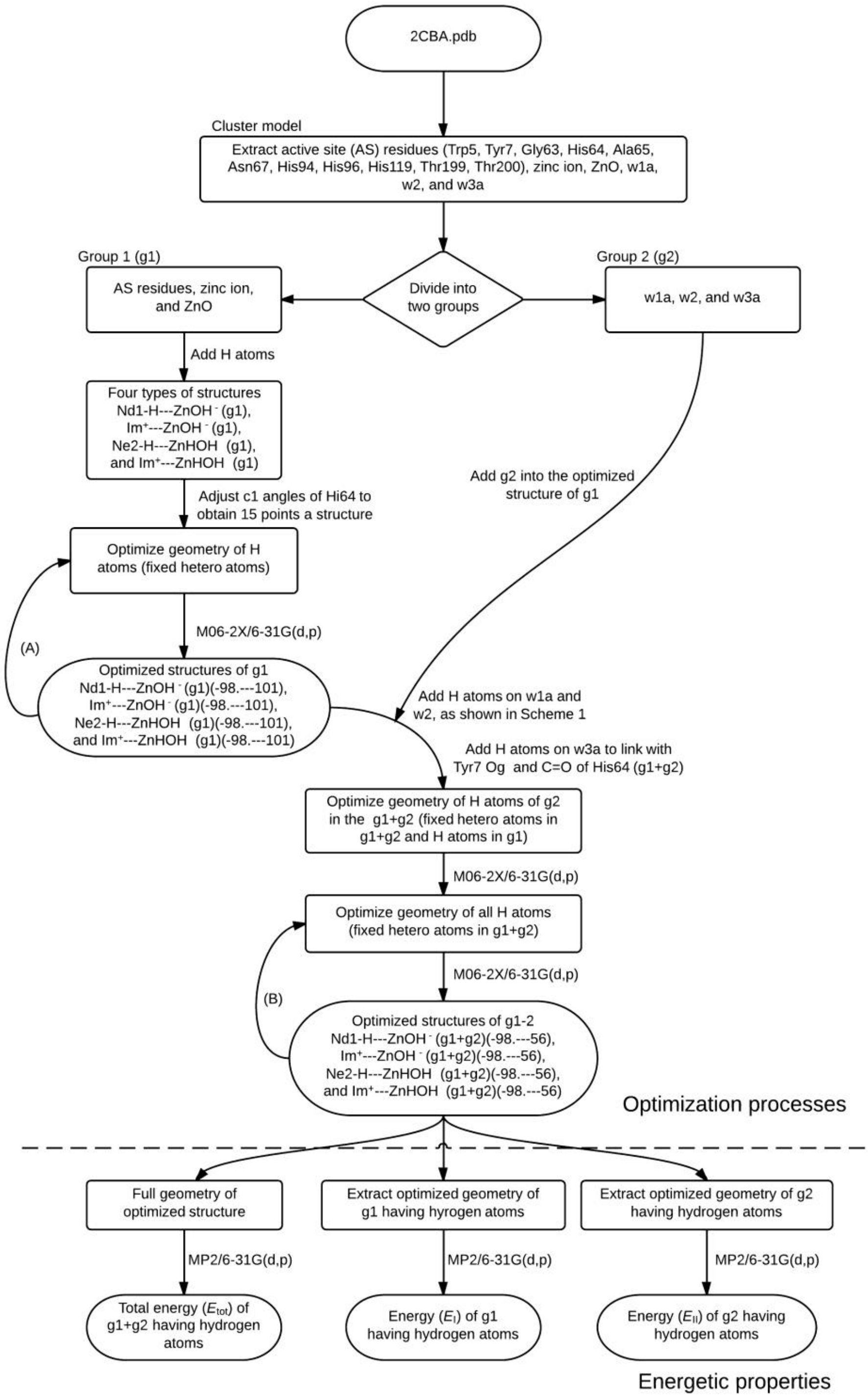
2CBA.pdb
Cluster model
Extract active site (AS) residues (Trp5, Tyr7, Gly63, His64, Ala65, Asn67, His94, His96, His119, Thr199, Thr200), zinc ion, ZnO, w1a, w2, and w3a
Group 1 (g1)
AS residues, zinc ion, and ZnO
Divide into two groups
Group 2 (g2)
w1a, w2, and w3a
Add H atoms
Four types of structures Nd1-H---ZnOH⁻ (g1), Im⁺---ZnOH⁻ (g1), Ne2-H---ZnHOH (g1), and Im⁺---ZnHOH (g1)
Adjust c1 angles of Hi64 to obtain 15 points a structure
Add g2 into the optimized structure of g1
Optimize geometry of H atoms (fixed hetero atoms)
M06-2X/6-31G(d,p)
(A)
Optimized structures of g1 Nd1-H---ZnOH⁻ (g1)(-98.---101), Im⁺---ZnOH⁻ (g1)(-98.---101), Ne2-H---ZnHOH (g1)(-98.---101), and Im⁺---ZnHOH (g1)(-98.---101)
Add H atoms on w1a and w2, as shown in Scheme 1
Add H atoms on w3a to link with Tyr7 Og and C=O of His64 (g1+g2)
Optimize geometry of H atoms of g2 in the g1+g2 (fixed hetero atoms in g1+g2 and H atoms in g1)
M06-2X/6-31G(d,p)
Optimize geometry of all H atoms (fixed hetero atoms in g1+g2)
M06-2X/6-31G(d,p)
(B)
Optimized structures of g1-2 Nd1-H---ZnOH⁻ (g1+g2)(-98.---56), Im⁺---ZnOH⁻ (g1+g2)(-98.---56), Ne2-H---ZnHOH (g1+g2)(-98.---56), and Im⁺---ZnHOH (g1+g2)(-98.---56)
Optimization processes
Full geometry of optimized structure
Extract optimized geometry of g1 having hyrogen atoms
Extract optimized geometry of g2 having hydrogen atoms
MP2/6-31G(d,p)
MP2/6-31G(d,p)
MP2/6-31G(d,p)
Total energy (Etot) of g1+g2 having hydrogen atoms
Energy (EI) of g1 having hydrogen atoms
Energy (EII) of g2 having hydrogen atoms
Energetic properties

Figure 16. The schematic process of geometry optimization for model structure.

A.3.2 Potential energy profiles

In order to compare the Nδ1-H tautomer, Nε2-H tautomer, and imidazolium ion form in one figure, the energy data of a buffer and its conjugate acid were added. The 3,5-lutidine was selected as a buffer molecule. The buffer energy data were added to Nδ1-H tautomer and imidazolium ion form. The conjugate acid energy data was added to the Nε2-H tautomer. Figure 17 (upper side) shows the energy profile of the structure without the hydrogen bond-bridge. The energy profile of Imi-ZnOH is the highest compared with the others, and the "out" conformation was more stable compared to the "in" conformation. Another two forms (Nδ1-ZnOH and Nε2-ZnOH2), has the "in" conformation more stable than "out" conformation. The barrier height was 7.6 kcal/mol, 5.5 kcal/mol, 9.4 kcal/mol for Nδ1-ZnOH, Nε2-ZnOH2 tautomer, and Imi-ZnOH respectively.

Figure 17 (lower side) shows the energy profile of each form, including hydrogen bond-bridge. The order of energy profiles was similar with the structure without water-bridge. However the stability of all forms tend to "in" conformation. The "in" conformation was stabilized by the hydrogen bond connection. This also caused the height of barrier increased to 12.7 kcal/mol for Nδ1-ZnOH, 4.2 kcal/mol for Nε2-$ZnOH_2$, and 15.5 kcal/mol for imi-ZnOH.

The energy barrier can be related to the transition rate theory, as shown in the following equation.

$$k_1 = \left(\frac{kT}{h}\right) exp\left(\frac{-\Delta G}{RT}\right) \tag{A.1}$$

Where k_1 is the rate of transmission in the approximation of the transition state theory limit, k is the Boltzmann constant, h is the Planck constant, ΔG is the energy barrier

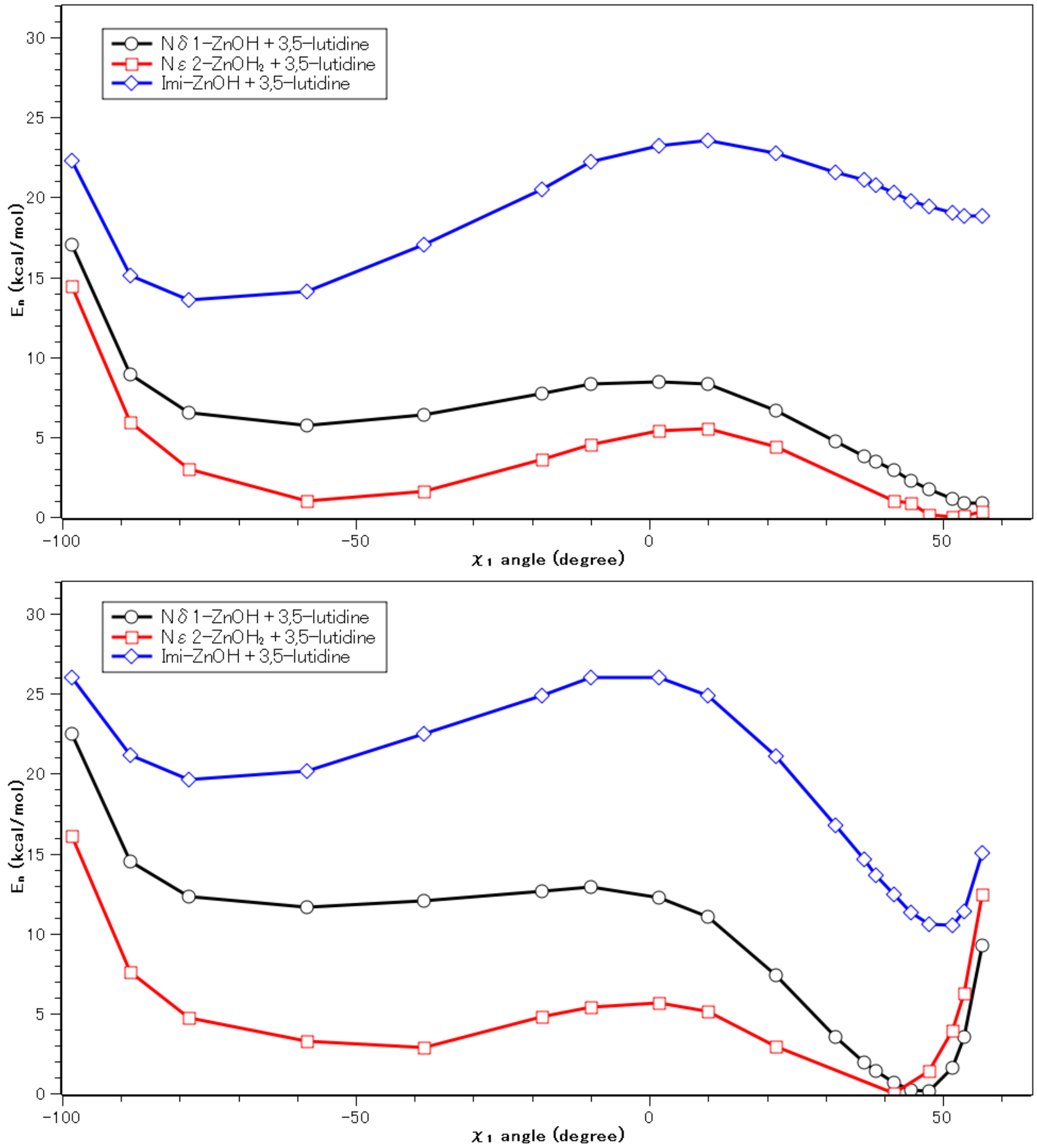

Figure 17. The energy profiles of Nδ1-ZnOH (black), Nε2-ZnOH2 (red), and Imi-ZnOH (blue) after adding energy of a buffer 3,5-lutidine for without hydrogen bond-bridge (upper side) and with hydrogen bond-bridge (lower side).

height, R is the gas constant, and T is temperature. HCAII has 10^6 s^{-1} maximal turnover rates, and assuming the temperature is 25°C, we can obtain the value of ΔG is 9.2 kcal/mol, which should be the maximum energy barrier in all basically catalytic processes. Our calculated energy barrier of rotational motion of His64 Nδ1-ZnOH and Imi-ZnOH is higher than 9.2 kcal/mol, which is not possible to rotation. Otherwise the Nε2-$ZnOH_2$ energy barrier was 4.2 kcal/mol, which is lower than maximal turnover. These results tentatively suggest that His64 does not have the rotational motion, but a flexible motion in the either “in” or “out” conformation.

A.4 Conclusion

We investigate the potential energy profile of large structure, including zinc atom, His64, hydrogen bond-bridge, and surrounding residues. The hydrogen bond-bridge affects the stabilization at the “in” conformation. The hydrogen bond-bridge help stabilize the structure at “in” conformation. The additional stabilization from hydrogen bond-bridge could restrict the rotational motion. However more research on this model structure is needed to explain the proton transfer process.

List of Publications

Paper Publications during 2011-2014 as the First Author:

1. **M. Koyimatu**, H. Shimahara, M. Iwayama, K. Sugimori, K. Kawaguchi, H. Saito, and H. Nagao, *Theoretical Model For Assessing Properties of Local Structures in Metalloprotein*, American Institute of Physics AIP Conference Proceeding, Volume 1518, pp. 626-629 (2013).
2. **Muhamad Koyimatu**, Hideto Shimahara, Kazutomo Kawaguchi, Hirosaki Saito, Kimikazu Sugimori, and Hidemi Nagao, *Theoretical Study of a π-stacking interaction in carbonic anhydrase*, Recent Development in Computational Science, Volume 4, pp. 87-93 (2013).
3. **Muhamad Koyimatu**, Hideto Shimahara, Kimikazu Sugimori, Kazutomo Kawaguchi, Hirosaki Saito, and Hidemi Nagao, *π-stacking Interaction between Heterocyclic Rings in a Reaction Field of Biological System*, The Physical Society of Japan JPS Conference Proceeding, Volume 1 (2014).

Other paper

1. Hideto Shimahara, Kimikazu Sugimori, Muhamad Koyimatu, Hidemi Nagao, Tadayasu Ohkubo, and Yuji Kobayashi, *An approach to water molecule dynamics associated with motion of catalytic moiety*, American Institute of Physics AIP Conference Proceeding, Volume 1518, pp. 610-613 (2013)

References

[1] R. Brinkman, R. Margaria, N. U. Meldrum and F. J. W. Roughton, "The CO2 catalyst present in Blood," *Journal Physiol,* vol. 75, pp. 3-4, 1932.

[2] W. C. Stadie and H. O'Brien, "The catalysis of the hydration of carbon dioxide and dehydration of carbonic acid by an enzyme isolated from red blood cells," *Journal of Biological Chemistry,* vol. 103, no. 2, pp. 521-529, 1933.

[3] N. U. Meldrum and F. J. Roughton, "Carbonic anhydrase. Its preparation and properties," *The Journal of physiology,* vol. 80, no. 2, pp. 113-142, 1993.

[4] J. R. G. Bradfield, "Plant Carbonic Anhydrase," *Nature,* vol. 159, p. 467, 1947.

[5] S. Lindskog, "Structure and mechanism of carbonic anhydrase," *Parhmacology & therapeutics,* vol. 74, no. 1, pp. 1-20, 1997.

[6] D. Keilin and T. Mann, "Carbonic anhydrase. Purification and nature of the enzyme," *Biochemical Journal,* vol. 34, no. 8-9, pp. 1163-1176, 1940.

[7] I. Simonsson, B. H. Jonsson and S. Lindskog, "C-13 NMR study of carbon dioxide-bicarbonate exchange catalyzed by human carbonic anhydrase C at chemical equilibrium.," *Eur. J. Chem,* vol. 93, pp. 409-417, 1979.

[8] D. N. Silverman, C. K. Tu, S. Lindskog and G. C. Wynns, "Rate of exchange of water from the active site of human carbonic anhydrase," *J. Am. Chem. Soc.,*

vol. 93, pp. 409-417, 1979.

[9] T. H. Maten, "Carbonic Anhydrase: chemistry, physiology, and inhibition," *Physiol. Rev.*, vol. 47, pp. 595-781, 1967.

[10] R. E. Tashian, "The carbonic anhydrase: widening prespectives on their evolution, expression and function," *BioEssays*, vol. 10, pp. 186-192, 1989.

[11] H. Steiner, B. H. Johnsson and S. Lindskog, "Catalitic mehanism of carbonic-anhydrase-hydrogen-isotope effect on kinetic parameter of human C isozyme," *Eur. J. Biochem*, vol. 59, pp. 253-259, 1975.

[12] C. K. Tu, D. N. Silverman, C. Forsman, B. H. Jonsson and S. Lindskog, "Role of histidine 64 in the catalytic mechanism of human carbonic anhydrase II studied with a site specific mutant," *Biochemistry*, vol. 28, pp. 7913-7918, 1989.

[13] K. Hakanson, M. Carlsson, L. Svensson and A. Lijas, "Structure of native and apo carbonic anhydrase II and structure of some of its anion-ligand complex," *J. Mol. Biol*, vol. 227, pp. 1192-1204, 1992.

[14] M. Blakeley, A. Mitschler, I. Hazemann, F. Meilleur, D. Myles and A. Podjarny, "Comparison of hydogen determination with X-ray and neutron crystallography in a homan aldose reductase-inhibitor complex.," *European Biophysics Journal*, vol. 35, pp. 577-583, 2006.

[15] H. Shimahara and e. al., "Tautomerism of Histidine 64 Associated with the Proton Transfer in Catalysis of Carbonic Anhydrase," *The Journal of Biological Chemistry*, vol. 282, no. 13, pp. 9646-9656, 2007.

[16] G. R. Desiraju and T. Steiner, The Weak Hydrogen Bond in Structural Chemistry and Biology, Oxford: Oxford University Press, 1999.

[17] S. Scheiner, Hydrogen Bonding. A theoretical Perspective, Oxford: Oxford University Press, 1997.

[18] G. A. Jeffrey and W. Saenger, Hydrogen Bonding in Biology and Chemistry, Berlin: Springer-Verlag, 1991.

[19] G. A. Jeffrey, An Introduction to Hydrogen Bonding, New York: Oxford University Press, 1997.

[20] D. Voet and J. G. Voet, Biochemistry, New York: John Wiley & Sons, Inc., 1995.

[21] W. S. Brey, Physical Chemistry and Its Biological Apllications, California: Academic Press, 1978.

[22] R. M. Dreizler and E. Engel, Density functional theory, Springer, 2011.

[23] P. Hohenberg and W. Kohn, "Inhomogeneous Electron Gas," *Phys. Rev.,* vol. 136, p. B 864, 1964.

[24] W. Kohn and L. J. Sham, "Self-consistent equations including exchange and correlation effects," *Phys. Rev.,* vol. 140, p. A 1133, 1965.

[25] S. H. Vosko, L. Wilk and M. Nusair, "Accurate spin-dependent electron liquid correlation energies for local spin density calculation: a critical analysis," *Canadian Journal of Physic,* vol. 58, no. 8, pp. 1200-1211, 1980.

[26] C. Lee, W. Yang and R. G. Parr, "Development of the Celle-Salvetti correlation-energy formula into a functional of the electron density," *Physycal Review B,* vol. 37, pp. 785-789, 1988.

[27] A. Becke, "Density-functional exchange-energy approximation with correct asymptotic behavior," *Phys. Rev. A,* vol. 38, no. 6, pp. 3098-3100, 1988.

[28] A. D. Becke, "Density-functional thermochemistry. III. The role of exact exchange," *The Journal of Chemical Physics,* vol. 98, no. 7, pp. 5648-5652, 1993.

[29] C. Møller and M. S. Plesset, "Note on an approximate treatment for many-electron systems," *Phys. Rev.,* vol. 46, pp. 618-622, 1934.

[30] Y. Zhao and D. G. Truhlar, "The M06 suite of density functionals for main group thermochemistry, thermochemical kinetics, noncovalent interactions, excited states, and transition elements," *Theor CHem Account,* vol. 120, pp. 215-241, 2008.

[31] Y. Zhao and D. G. Truhlar, "A new local density functional for main-group thermochemistry, transition metal bonding, thermochemical kinetics, and noncovalent interactions," *Journal of Chemical Physics,* vol. 125, 2006.

[32] J. P. Perdew, K. Burke and M. Ernzerhof, "Generalized Gradient Approximation Made Simple," *Phys. Rev. Lett.,* vol. 77, no. 18, pp. 3865-3868, 1996.

[33] J. Jaramillo and G. E. Scuseria, "Assessment of the Van Voorhis-Scuseria exchange-correlation functional for predicting excitation energies using time-dependent density functional theory," *Theor. Chem. Acc.,* vol. 105, pp. 62-67,

2000.

[34] C. A. Hunter and J. K. M. Sanders, "The nature of pi-pi Interactions," *J. Am. Soc.,* vol. 112, pp. 5525-5534, 1990.

[35] Gaussian 09, Revision **D.01**, M. J. Frisch, G. W. Trucks, H. B. Schlegel, G. E. Scuseria, M. A. Robb, J. R. Cheeseman, G. Scalmani, V. Barone, B. Mennucci, G. A. Petersson, H. Nakatsuji, M. Caricato, X. Li, H. P. Hratchian, A. F. Izmaylov, J. Bloino, G. Zheng, J. L. Sonnenberg, M. Hada, M. Ehara, K. Toyota, R. Fukuda, J. Hasegawa, M. Ishida, T. Nakajima, Y. Honda, O. Kitao, H. Nakai, T. Vreven, J. A. Montgomery, Jr., J. E. Peralta, F. Ogliaro, M. Bearpark, J. J. Heyd, E. Brothers, K. N. Kudin, V. N. Staroverov, R. Kobayashi, J. Normand, K. Raghavachari, A. Rendell, J. C. Burant, S. S. Iyengar, J. Tomasi, M. Cossi, N. Rega, J. M. Millam, M. Klene, J. E. Knox, J. B. Cross, V. Bakken, C. Adamo, J. Jaramillo, R. Gomperts, R. E. Stratmann, O. Yazyev, A. J. Austin, R. Cammi, C. Pomelli, J. W. Ochterski, R. L. Martin, K. Morokuma, V. G. Zakrzewski, G. A. Voth, P. Salvador, J. J. Dannenberg, S. Dapprich, A. D. Daniels, Ö. Farkas, J. B. Foresman, J. V. Ortiz, J. Cioslowski, and D. J. Fox, Gaussian, Inc., Wallingford CT, 2009.

[36] C. Maupin and G. A. Voth, "Preferred orientation of His64 in human carbonic anhydrase II," *Biochemistry,* vol. 46, pp. 2938-2947, 2007.

[37] H. B. Jansen and P. Ros, "Non-empirical molecular orbital calculations in the protonation of carbon monoxide," *Chemical Physics Letters,* vol. 3, no. 3, pp. 140-143, 1969.

[38] B. Liu and A. D. McLean, "Accurate calculation of the atrractive interaction of two ground state helium atoms," *The Journal of Chemical Physics,* vol. 59, no. 8, pp. 4557-4558, 1973.

[39] S. Nair and D. Christianson, "Unexpected pH-Dependent COnformation of His-64, the Proton Shuttle of Carbonic Anhydrase," *J. Am. Chem. Soc.,* vol. 113, pp. 9455-9458, 1991.